PERFORMANCE ANALYSIS OF UNDERWATER WIRELESS OPTICAL COMMUNICATION SYSTEM(UWOC)

Submitted in partial fulfilment of the requirements for the degree of

Bachelor of Technology

in

Electronics and Communication Engineering

by

BALACHANDIRAN KAILASH	**-**	**16BEC0709**
MANISH PAULSON	**-**	**16BEC0712**
SAPARI AV	**-**	**16BEC0599**

Under the guidance of
Prof. Dr. Sangeetha A
School of Electronics Engineering,
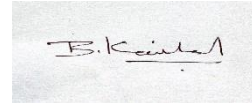## Vellore Institute of Technology,
Vellore.

May, 2020

<u>DECLARATION</u>

We as a result of this declare that the thesis entitled "PERFORMANCE ANALYSIS OF UNDERWATER WIRELESS OPTICAL COMMUNICATION SYSTEM(UWOC)" submitted by BALACHANDIRAN KAILASH, MANISH PAULSON, SAPARI AV for the award of the degree of *Bachelor of Technology in Electronics and Communication Engineering* to Vellore Institute of Technology is a record of bonafide work carried out by us under the supervision of Prof. Dr. Sangeetha A.

We further declare that the work reported in this thesis has not been submitted and will not be submitted, either in part or in full, for the award of any other degree or diploma in this institute or any other institute or University.

BALACHANDIRAN KAILASH

Place : Vellore

Date : 25/05/2020

MANISH PAULSON

SAPARI AV

Signature of the candidate

CERTIFICATE

This is to certify that the thesis entitled "PERFORMANCE ANALYSIS OF UNDERWATER WIRELESS OPTICAL COMMUNICATION SYSTEM(UWOC)" submitted by BALACHANDIRAN KAILASH, MANISH PAULSON, SAPARI AV, School of Electronics Engineering, Vellore Institute of Technology, for the award of the degree of *Bachelor of Technology in Communication Engineering*, is a record of bonafide work carried out by him under my supervision, as per the VIT code of academic and research ethics.

      The contents of this report have not been submitted and will not be submitted in part or in full, for the award of any other degree or diploma in this institute or any other institute or University. The thesis fulfils the requirements and regulations of the University and, in any opinion, meets the necessary standards for submission.

Place : Vellore

Date : 25/05/2020   **Prof. Dr. Sangeetha A**

                                           Signature of the Guide

The thesis is satisfactory/unsatisfactory

Internal Examiner   **External Examiner**

Approved by

Dr. Thanikaiselvan V,

Head of Department,

Electronics and Communication Engineering.

ACKNOWLEDGEMENT

First of all, we would like to express our deep sense of respect and gratitude towards our advisor and guide Prof. Dr. Sangeetha A, who has been the guiding force behind this Project work. We're greatly indebted to her and for her constant encouragement, invaluable advice, and for propelling us further in every aspect of our academic life. Her presence and optimism have provided an invaluable influence on our career and outlook for the future. We consider it our good fortune to have got an opportunity to work with such a wonderful person.

We would like to thank all faculty members and staff of the Department of Electronics and Communication Engineering, Vellore Institute of Technology, for their generous help in various ways for the completion of this Project Work.

We would like to thank all our friends and especially our classmates for all the thoughtful and mind-stimulating discussions we had, which prompted us to think beyond the obvious. We're especially indebted to our parents for their love, sacrifice, and support. They are first teachers after we came to this world and have set great examples for us about how to live, study and work.

Finally, we extend my gratefulness to all those who are directly or indirectly involved in this project work.

BALACHANDIRAN KAILASH

MANISH PAULSON

SAPARI AV

Executive Summary

We know that Underwater optical wireless communication (UOWC) systems have been receiving a great deal of attention because of their advantages of higher data rates, lower latency, and security while comparing it to the traditional acoustic communications. However, the problem with the underwater optical wireless communication is that the transmitting length is relatively short compared to acoustic communication. It is because the light beam in the channel suffers from absorption, scattering, and the turbulence fading of the water channel. Despite these drawbacks, UOWC is still one of the promising technology. Moreover, it is also crucial to use this water as a channel because we know that our earth is around 75% covered with water. Thus exploring this UOWC to its full potential has become essential for our effective communication.

In this project, we have been exploring how can different modulation techniques like QAM-OFDM and PSK-OFDM with different orders, along with varying methods of encoding effects the transmitting length of the signal and also how the unusual combination of modulation and encoding techniques affects the Bit error rate (BER) of the receiving signals. At the end of this project, we can conclude that which combinations of modulation techniques, along with encoding the error detection and correction, provide great transmitting lengths and lower bit error rates (BER).

CONTENTS

Page No.

List of Figures

List of Tables

List of Abbreviations

Abbreviation	Definition
AWGN	Additive White Gaussian Noise
SNR	Signal to Noise Ratio
BW	Bandwidth
OFDM	Orthogonal Frequency Division Multiplexing
PSK	Phase Shift Keying
QAM	Quadrature Amplitude Modulation
BER	Bit Error rate
ISI	Inter Symbol Interference
LDPC	Low-Density Parity-Check Code
BCH	Bose–Chaudhuri–Hocquenghem
CEAPF	Combination of Exponential and Arbitrary Power Function
WDGF	Weighted double gamma function
FOV	Field of view
DGF	Double gamma function

Symbols and Notations

A	Wavelength
h	Planck's Constant
c	Velocity of Light
E_g	Energy Gap
F_c	Cut-off frequency
η	Quantum Efficiency
q	Electron Charge
T	Temperature
B	Bandwidth
K	Boltzmann Constant

1.INTRODUCTION

1.1 OBJECTIVE

The primary objective of this project is to simulate an impulse function for an underwater wireless channel for different Field of Views (FOV) with primary factors affecting the channel are scattering and absorption. From the simulated impulse function, we use different kinds of mapping schemes, namely OFDM with 4-QAM, 16-QAM, and OFDM with 4-PSK, 16-PSK, and record Bit error rate (BER) of these different signals and analyze and compare their performance. Moreover, we analyze the maximum distance that can be achieved by the transmitted signal. And to reduce the bit error rate, we deploy different encoding techniques such as LDPC and BCH encoding and try to minimize the bit error rate of the received signal.

1.2 MOTIVATION

Around 75% of the earth is covered with water. It contains a large number of natural resources, and hence for exploring these resources, the development of an effective underwater wireless communication system became very important. Due to several applications like scientific marine exploration, voice and data communications between drivers, mine surveillance, the study of disasters and military projects, fields of underwater wireless optical communication is rapidly increasing. For example, ocean monitoring, ocean exploration, undersea expeditions. So, it is one of the vital communication media for communication researchers.

Most of the papers published on the underwater wireless channel are based on adding noise to the channel, such as white Gaussian noise. The results simulated are also in the form of BER vs SNR. The results generated from these systems do not account for varying lengths, absorption, and scattering coefficients. Thus, these systems are never the best depiction of a UWOC. DGFs were first adopted to model the impulse response in the cloud. Inspired by the dispersive nature of both cloud and underwater channels, Tang applied DGFs to model the impulse response in UWOC links. However, these functions are only applicable with relatively large values of attenuation length. To generalize these functions, Dong added two parameters to the DGFs and proposed the weighted double gamma functions (WDGF) [1].

 However, current acoustic communication technologies can only provide limited data rates due to the narrow bandwidth available as well as extended multipath spreading in the underwater channel. Underwater wireless optical communication (UOWC) systems have received a great deal of attention due to the advantages of a much higher data rate, security, and much lower latency compared to the traditional underwater acoustic communication systems. Electromagnetic (EM) waves, in the radiofrequency (RF) range, is a good option for underwater wireless communication when used for high data rate transfer in short distances. The speed of EM waves mainly depends upon permeability(μ), permittivity(ϵ), conductivity(σ) and volume charge density(ρ) which varies according to the type of underwater conditions and frequency be infused. It has been observed that the attenuation of RF waves increases with the increase in rate and is heavily attenuated by seawater [2]. Optical waves, on the other hand, have high bandwidth, but they are affected by other propagation effects due to temperature fluctuations, scattering, dispersion, and beam steering. Wireless underwater communication is

limited to short distances due to severe water absorption at optical frequency band, and strong backscatter from suspended particles. However, there is a relatively low attenuation optical window of blue-green wavelengths of the EM spectrum underwater.

For this reason, UOWC has observed a surge in interest from the development of blue-green sources and detectors. The blue-green wavelengths are capable of proving high bandwidth communication over moderate ranges (up to 100s of meters). Although the transmit length is relatively short as the light beam suffers from absorption, scattering, and turbulence-induced fading, UOWC is still a promising technology in many applications. Still, UWOC is not used to its full capability. Even today, it is UNEXPLORED in many areas. Therefore, working on this topic will be more useful for us as students and contribute our work towards this part of the communication system.

1.3 LITERATURE SURVEY

Brandon Cochenour et al. (2006). Recent interest in ocean exploration has motivated us to develop wireless communication techniques in this challenging environment. A radio frequency (RF) carrier is not the preferred choice due to its high attenuation in water. Although acoustic techniques have made tremendous progress in establishing wireless underwater links, yet they are limited in bandwidth. A third option is optical radiation, which is discussed in this paper. The transmission of the optical carrier is highly dependent on water type. This is one of the main drawbacks of the underwater wireless optical communication system. This paper presents some of the challenges in applying an optical link in turbid water environments and tries to answer how water clarity affects the overall link. The studies on optical properties of water are rarely considered from the standpoint of implementing a laser communication link. The reviews on the feasibility of underwater wireless optical communications done in the past decades are incomplete. They were performed in clean water, and the transmitter power was varied to simulate attenuation due to the environment. The real effect of water turbidity on link range, data rate, and pointing accuracy is still unknown. This experimental work tries to fill this void.

In this work, they investigated the effects of multiple scattering in turbid environments on a modulated optical signal for implementing wireless underwater communication links. In the preliminary experiments, the recovery of the RF sub-carrier was mostly unaffected by water purity. Changes in the absolute phase of the recovered RF envelope against the increasing water turbidity confirms that multiple scattering is occurring. However, unlike acoustic systems, the multipath effects are static during the acquisition time. This was supported when short data bursts were detected error-free at a rate of 1Mbps [3].

Hou Pin Yoong et al. (2009). This paper deals with the modeling of the seawater acoustic channel to obtain the optimum carrier frequency for an autonomous underwater vehicle (AUV) wireless communication system. The wireless communication distance of an AUV with its control vessel changes due to the changes due to the mission at different depths. THE current AUV is designed with an operating depth of 0 to 2000m. Therefore, the existing model had a

limitation when the operational depth varies based on the mission assignment. This is because of the optimum frequency to noise ratio changes for the transmission distance. This paper provides us with a method to determine the optimum carrier frequency for the AUV wireless communication system to overcome the existing way of modeling. The mathematical model made with the noise, distance, and the rate is formulated, and the optimum frequencies at various intervals are set through simulation. The average frequency is said to be the optimum transmission carrier frequency from the frequency band. The determined rate can be further utilized for hardware improvements.

The primary purpose of this paper is to present an innovative method to start upon. They deal with the different characteristics between acoustic waves and electromagnetic waves in underwater wireless communication. The paper describes the steps in modeling the formulation of the seawater channel. The simulation results and method of obtaining the optimal carry frequency are discussed in the paper. It also provides us with a clear-cut conclusion on the paper. The carrier frequency and Doppler Effect are obtained based on the works of this paper. The next step will be defining the number of channels needed for the transmission, followed by the transmission power study, and lastly, building the hardware for realizing the underwater wireless communication system [4].

P Vijaya Kumar et al. (2011). They have presented three scenarios in this paper regarding UWOC. They are a) Line of sight (LOS) b) Modulating Retro Reflector link c) Reflective link. This analysis, each case is tested with water having different extinction coefficient and various noise backgrounds. In this paper, they have analyzed these links in OPTI SYSTEM. It is a software design tool that is innovative, rapidly evolving, and powerful. It enables the users to plan, test, and simulate most types of optical links in the transmission layer of a broad spectrum of optical networks from LAN, SAN, and MAN to ultra-long-haul. It offers the design and planning of transmission layer optical communication from component to the system level, and present the analysis and scenarios visually. They concluded that the line of sight scenario is most effective than the other two. The results of their works indicate that there are losses at the receiver end for medium distances. From this, we can see that as the water's turbidity increases, the water absorption also rises. So the losses at the receiver also increase. Thus the communication in turbid harbour water reduces the data rate and results in ineffective communication [5].

Abd El-Naser A. Mohamed et al. (2012). This paper's primary focus is to construct an underwater link budget, which includes the effects of scattering and absorption of realistic seawater. They have also developed the underwater optical wireless communication systems to have shorter ranges as well. It can provide higher bandwidth (up to several hundred Mbit/sec) communications with the assistance of new high brightness blue LED sources. High-speed optical links can be viable for short-range applications, as suggested by laser diodes. Optical wireless systems are based on free-space optics technology. Free space optical communications is a line of sight (LOS) technology. It transmits a modulated beam of visible or infrared light through the atmosphere or, as in our study, concerning on wireless system underwater for broadband communications. This is regarded as one of the most promising approaches for addressing the emerging broadband access market. It offers many features, principal among

them being a low start-up and operational costs, rapid deployment, and high fiber link bandwidth. Wireless optical communications under water-primarily deployed where performance, security, rapid deployment, and cost-savings are critical issues. It is observed that the increased operating optical signal wavelength, resulting in the increased SNR and the decreased BER, transmitted signal bandwidth, and received signal power for both short and very short ranges under considerations. As well as it is theoretically found that the increased both receiver aperture diameter and operating optical signal wavelength, and the decreased half-angle transmitter beam width, lead to the increased SNR and the decreased BER for both short and very short ranges under study. Moreover, we have observed that the increased both operating optical signal wavelength and transmission, resulting in the decreased transmitted signal bandwidth for both wireless ranges under the same operating parameters. Finally, it is indicated that the short wireless range has presented higher PR, SNR, and BW_{sig} and lower BER compared to the short wireless range [6].

Mohammad-Ali Khalighi et al. (2014). This paper reviews the recent research works on Underwater Wireless Optical Communication and the available commercialized systems and provides a performance study of a typical UWOC system under some simplifying assumptions for system modeling. It also discusses the issues and challenges faced by the UWOC system. It also discusses the impact of link misalignment, modulation schemes, and error correction codes used in UWOC. It also provides directions for future research on these UWOC systems. Currently, there is a lack of channel models that include turbulence in an accurate way. The main difficulty of developing such models is because turbulence highly depends on the operational scenario and water conditions. The design of appropriate signaling techniques adapted to the aquatic channel is something to be explored. It also emphasizes on the need to mitigate link misalignment. As power consumption is an essential issue in UWOC, they had to minimize the intensity loss by reducing its beam divergence. This paper also discusses the advantages of underwater wireless optical communication over the currently used systems [7].

Prashant Kumar et al. (2015). This paper talks about the recent findings in the area of Underwater Acoustic communication related to multi-carrier communication and mainly to orthogonal frequency division multiplexing (OFDM) for applied, theoretical and simulation studies. An attempt has been made to present a compact yet exhaustive literature survey that will serve as a standard reference for researchers working in the area. Stress has been laid on the physical layer issues as it works as the necessary foundation of any network. The focus areas of research activities have been identified, and a summary of the ongoing operations and future trends has been presented.

This review paper aims at supplementing the underwater communication literature with a summary of all the recent advances and introduce the readers to the challenges and provide an insight into some of the open research problems which need to be solved shortly. The rest of the section is organized as follows. The second section discusses the typical characteristics of the underwater channel. The third section examines the suitability of multi-carrier communication for the Underwater Acoustic channel and explores some of the variants of OFDM applied to such channels. The fourth section of the paper summarizes the diversity schemes used to multi-carrier underwater acoustic communication. The fifth section reviews

CDMA based multi-carrier techniques and multiuser issues in underwater acoustic communications, and the final section reviews channel estimation and equalization techniques for underwater acoustic multi-carrier communication. Finally, the authors summarize the trends and identify some challenging problems that need the research community's attention. The research's main focus areas are underwater channel modeling, an empirical model for the noise of the underwater acoustic channel, and adaptive modulation techniques. This paper reviewed the recent development in multi-carrier underwater acoustic communications with an emphasis on the physical layer [8].

S Anandalatchoumy et al. (2015). This paper describes the characteristics of the acoustic propagation in detail, and channel models based on the various propagation phenomena in shallow water channels and deep-water channels. The transmission losses that have occurred in each model are thoroughly investigated. It carefully analyzes the signal to noise ratio (SNR) at the receiver. The numerical results obtained from the analytical simulations carried out in MATLAB shows the critical issues to be considered to develop suitable communication protocols for Underwater Wireless Communication Networks to provide useful and good communication.

This paper provides a comprehensive study on the acoustic propagation characteristics and acoustic channel models with detailed discussions on the design issues and the challenges of effective communication in an underwater environment. This paper is classified into six sections, as shown below. The second section discusses some of the current research findings related to the acoustic channel models. The following section inclines on the fundamental aspects and propagation characteristics of ocean acoustics and the underwater acoustic channel. The fourth section of the paper talks about the transmission losses incurred in shallow and deep-water channel and ambient noise in the ocean. The next section deals with the signal to noise ratio at the receiver and the final section provides us with a conclusion on the paper highlighting the critical considerations for the design of Underwater Wireless Communication Networks for effective communication. Underwater acoustic channel models for each mode of propagation in deep water and shallow water have been presented based on the studies on acoustic propagation characteristics. These studies show that attenuation increases with frequency. Therefore, short-range systems have high bandwidth, and long-range systems have low bandwidth. The desired communication range is determined by the distance between transceivers and the requirements of specific applications. The ambient noise is dependent on the selected frequency. Of all the six underlying propagation phenomena of sound in deep water, transmission length is very much lower within the convergence zone, providing suggestions for the optimal deployment of source and receiver nodes in underwater communication networks. Also, SNR for both cases is thoroughly analyzed [9].

V K Jagadeesh et al. (2015). This paper discusses the non-line of sight underwater wireless optical communication systems with multiple scattering, and the Monte Carlo simulation is applied to find the system's performance. The Henyey-Greenstein method models the distribution scattering angle of photons. For different water types, the average bit error rate is calculated using the on-off keying modulation.

In this paper, NLOS underwater optical wireless communication system based on multiple scattering of photos is proposed on different types of water, such as pure, clear, and coastal. Unless in the conventional methods, we dealt with multiple scattering models for NLOS propagation. Also, the distance traveled by photos in each type of water is compared in terms of BER for LOS and NLOS models. As can be expected, the NLOS has less transmission range compared to LOS for a specific BER. The perfectly aligned LOS model is always not possible in practice due to beam blockage caused by bubbles, fish, or large suspended particles. So this work is a critical phase, based on which NLOS underwater wireless communication can proceed [10].

Camila.M.G.Gussen et al. (2016). This paper discusses the different underwater wireless communication technologies. There are mainly three technologies available for underwater wireless transmissions – Radio Frequency communication, Optical transmission, and Acoustic Communication. Radio Frequency communication features high data throughput at short range and suffers from mild Doppler Effect. Optical transmission works in blue-green wavelength and requires line-of-sight positioning. Acoustic communication has low performance and is highly impaired by Doppler effects, but provides the most extended range of underwater communication. It also surveys the main features of these communication technologies. This paper provides us with the pros and cons of each of these three technologies. They also discuss the role of signal processing for the improvement of underwater communication. As expected, each communication technology requires distinct channel modeling, turning the task of conceiving a network employing flexible modems more challenging. This paper contributes to this direction by providing an up-to-date survey of the leading technical aspects and research challenges of wireless underwater communications [11].

Hemani Kaushal et al. (2016). This paper's primary focus is on the feasibility and reliability of high data rate underwater optical links due to various propagation phenomena that affect the system's performance. This paper also discusses the recent advancement in underwater wireless communication, Channel characterization, different modulation schemes, coding techniques, and various sources of noise specific to underwater optical wireless communication. Future scopes and the need for the development of new ideas in the field of underwater communication has been discussed. The paper also discusses the technologies that improve the UOWC system's efficiency, such as the hybrid acoustic-optic system and cooperative diversity, which not only provides an energy-efficient system but also enhances the capacity and range for the applications. This survey aims to determine the UOWC system's performance for a variety of underwater environments and develop a realistic system design model for underwater optical channels. This paper provides the readers with a reliable and coherent underwater optical channel and its research challenges. It develops a unique literature taxonomy of various lasers operating in the blue-green spectrum. It has been successful in providing graphical representations to enhance the understanding of the concept and discussing different challenges for underwater optical communication. Thus, the authors conclude that though acoustic waves are the robust and feasible carrier in today's scenario with rapid technological development and active ongoing research in UOWC, this technology will be more promising with game-changing potentials soon [12].

1.4 BACKGROUND

1.4.1 The Underwater wireless optical channel

The underwater environment is a very harsh and dynamically changing communication channel. The optical properties seawater is strongly affected by absorption, scattering, and turbulence. As a consequence, the optical beam propagating in water experiences angular spreading, deflection from the optical path, and amplitude and phase distortions. Besides, the transmitter beam is collimated with a minimal diameter leading to unavoidable link misalignments. These phenomena ultimately translate to low SNR and poor BER performance. Attenuation, which is a combined effect of absorption, and scattering is the leading cause of light loss in water. Absorption is the process in which the photon energy is lost due to the transfer of power during the interaction with water molecules, dissolved organic matters, and particles. In scattering, the photons are scattered away from the original path after interacting with particulate matter in the water. Scattering may cause temporal beam spreading, which results in inter-symbol interference (ISI) and degrades system BER performance. As a consequence, underwater wireless optical links are limited to much shorter ranges when compared to acoustics. The link range varies from a few meters in more turbid harbour waters to approximately 100 m in clear blue ocean waters. Spectral absorption coefficient (λ) and spectral scattering coefficient $b(\lambda)$ are the main IOPs that contribute to power loss between an optical transmitter and receiver in an underwater link. The combined effect of these two processes represents the total beam attenuation coefficient [13-18].

$$c(\lambda) = a(\lambda) + b(\lambda). \tag{1}$$

1.4.2 UWOC Channel Modelling

The presence of oceanic turbulences often perturbs the propagation of optical signals in seawater. Therefore, a detailed understanding of the underwater wireless optical channel is of paramount importance. The underwater channel needs to be fully characterized and statistically modeled to design robust and reliable UWOC systems. The underwater wireless optical channel can be of two kinds – turbulent and non-turbulent. A non-turbulent underwater channel is characterized by a water body where its salinity, temperature, and density are all uniform throughout the channel. Whereas a turbulent water channel is defined as a water column in which the refractive index of water changes due to temperature fluctuations, salinity variations, or the presence of air bubbles throughout the channel. In non-turbulent channels, the crucial phenomena that affect the propagation of light are absorption and scattering. In the case of absorption, some of the energy of the incident laser beam is dissipated along the UWOC link resulting in a reduced optical power at the receiver. Meanwhile, scattering creates dispersion, which introduces the temporal spread of beam pulse (inter-symbol interference) to the data communication. The total combination of scattering and absorption constitutes the total attenuation, which reduces the overall signal to noise ratio of the communication system. For longer transmission ranges for different water types. We take practical system parameters into account, particularly concerning the transmitter and the receiver, and consider more realistic water parameters. We do not take into account light polarization because we believe intensity

modulation with non-coherent detection, which is usually used in most systems due to its simplicity. Here we present channel impulse responses and quantify the channel time dispersion, especially by considering different receiver aperture sizes [17-23].

1.4.3 Numerical study of light transmission in water

As light propagates in water, absorption and scattering are two dominant impairing phenomena. The energy loss caused by absorption and scattering is generally evaluated by the absorption coefficient and scattering coefficient b, respectively. We can further use the extinction coefficient c as defined by Eq(1).To describe the total effect on energy loss. The values of a, b and c vary with the water type and light's wavelength λ. As a common practice, for simplicity, water types are modelled by waters with different values of chlorophyll concentration C. Thus, b and a can be modelled as a function of λ and C [21-25].

1.4.4 Effect of water on the Optical Beam

The two main processes affecting light propagation in water are absorption and scattering, which both depend on wavelength λ. Absorption is the irreversible loss of intensity and depends on the water's index of refraction. The spectral absorption coefficient (λ) is the main intrinsic optical property (IOP) to model water absorption. Scattering, on the other hand, refers to the deflection of light from the original path, which can be caused by particles of a size comparable to λ (diffraction), or by particulate matters with refraction index different from that of the water (refraction)[22-29].

1.4.5 Water Particles

In addition to water molecules, different particles in solution and suspension in water affect absorption and scattering. The spectral absorption coefficient a, and the scattering coefficient b can be calculated by adding the contribution of each class of particles to the pure seawater's corresponding factors. In particular, phytoplankton's determine the optical properties of most oceanic waters.

Knowing that underwater matters and the water quality are variant from one region to another, there are four major water types

• **Coastal waters:** They have a much higher concentration of planktonic matters, detritus, and mineral components that affect absorption and scattering.

• **Turbid harbour water:** They have a very high level of dissolved and in-suspension issues.

Table.1.1   Typical Coefficients for Different water types

Water type	C (mg/m^3)	a(m^{-1})	b(m^{-1})	c(m^{-1})
Coastal	0.83	0.088	0.216	0.305
Harbour	5.9	0.295	1.875	2.17

Their chlorophyll and related pigments strongly absorb light in the blue and red spectral ranges. We were interested to see the impact of C on the absorption and scattering properties of water. We notice that an increase in C has little effect on a, but it affects b considerably [13-29].

2. PROJECT DESCRIPTION AND GOALS

2.1 GOALS:

We transmit different kinds of signals from this simulated impulse function, namely OFDM with 4-QAM, 16-QAM and 4-PSK, 16-PSK, and record Bit error rate(BER) of these different signals and analyse their performance. And also, we analyse the maximum distance that can be achieved by the transmitted signal. To reduce the bit error rate, we use different encoding techniques such as LDPC, RS, and BCH Encoding and try to minimize the bit error rate of the received signal.

2.2 OFDM Transmitter

2.2.1 OFDM Signal Generation

OFDM uses multiple sub-carriers for data transmission. In this transmission scheme, all the sub-carriers are orthogonal to each other. OFDM is the combination of multi-carrier modulation and multiplexing, i.e., it is the process of digital mapping data on multiple carrier frequencies sharing bandwidth with other independent channels. In this modulation technique, data symbols modulate the orthogonally separated sub-carriers. The method is similar to the FDM technique except that the N non-overlapping sub-carriers signals are made orthogonal. Unlike other conventional frequency multiplexing techniques, it overcomes bandwidth wastage by using overlapping but orthogonal sub-carriers. This eliminates the use of guard bands on either side of each sub-carrier. If T is the symbol length, orthogonality between carriers is maintained by keeping minimum spacing of 1/T between subcarrier frequencies. OFDM has been an effective technique to compete for multipath fading in many areas of wireless communications. It is used for HF radio applications and has been chosen as the standard for digital audio broadcasting, digital terrestrial TV broadcasting, and wireless local area network. OFDM has been of critical interest for both wire line-based and wireless applications since it has high data rate transmission capability and robustness to multipath delay spread.

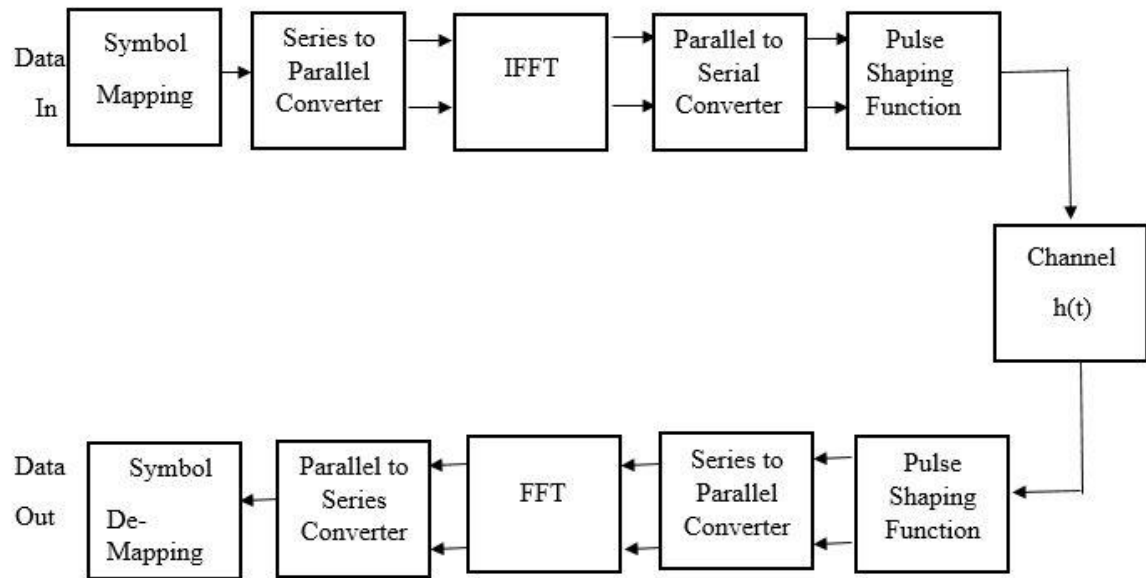Fig 2.1 OFDM Functional Block Diagram

2.2.2 Orthogonal Frequency Division Multiplexing block diagram:

The generic block diagram of an OFDM based transmitter and receiver digital communication system is shown in the figure. The different parts of the OFDM system are described in the thesis.
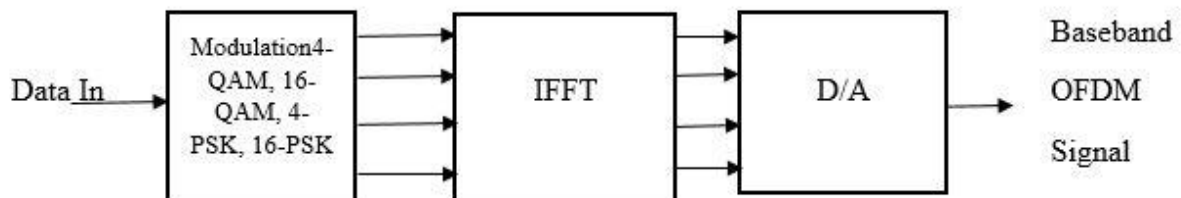

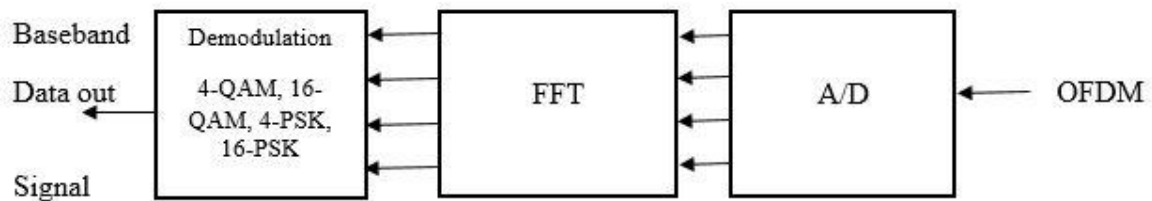Fig. 2.2 Transmitter Block Diagram

Fig. 2.3 Receiver Block Diagram

2.2.3. Addition of Cyclic Prefix

To this OFDM signal, a cyclic prefix is appended to avoid power loss due to echoes. It is generated by prefixing a symbol with its last samples. An important point to be considered to serve effectively in its length. The length of the cyclic prefix should be at least equal to the delay of its multipath channel. Apart from this, it retains sinusoids properties.
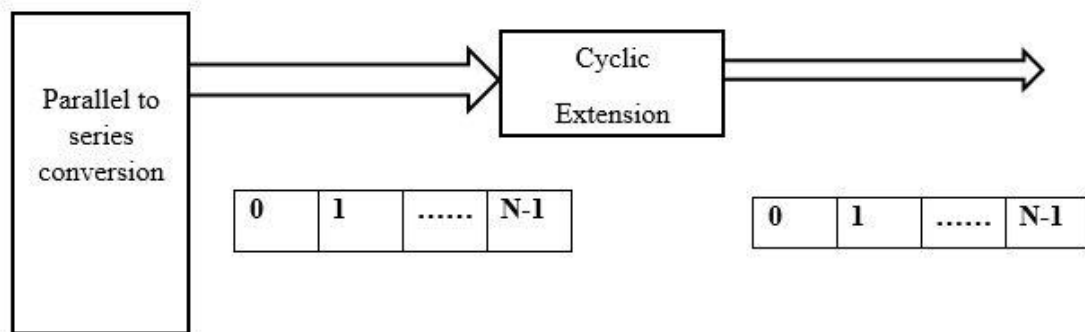
Fig. 2.4 Cyclic Extension Block

This is obtained after multiplexing, all the N symbols are together one after the other, but in case of the extended OFDM signal, there are samples appended to each symbol. Thereby the two successive symbols do not interfere with each other.

2.2.4 Advantages of OFDM

Some of the advantages of the OFDM signal include robustness in a multipath propagation environment and good tolerance to delay spread, resulting from the use of large number subcarrier and longer symbol duration compared to slow spread.

Advantages of OFDM:

- High Spectral efficiency due to overlapped spacing of subcarrier
- Efficient digital realization using the FFT technique.
- Eliminate ISI and ICI through use of cyclic prefix, thus reduced receiver complexity
- Channel Equalization becomes more natural by using adaptive equalization techniques in the frequency domain.
- Different modulation scheme can be applied to different subcarriers, allowing to adapt to the varying channel condition.
- By using channel coding and interleaving techniques, symbols lost due to deep fading can be recovered.

Disadvantages of OFDM

- The main disadvantage of OFDM is the high Peak to Average Power Ratio (PAPR), which requires a highly linear power amplifier, without which performance degradation happens due to out of band power enhancement.
- Sensitivity to Doppler shift
- Accurate frequency synchronization is needed; even a smaller offset in carrier clock leads to strong ICI due to the overlapped position of subcarrier.
- Loss inefficiency caused by cyclic prefix or guard interval,
- Since the advantages outweigh the disadvantages, OFDM has become the preferred choice for modern wireless communication.

2.2.5. OFDM Receiver

The first and foremost step at the receiver is to remove the appended cyclic prefix, which is equivalent to the removal of the guard interval.

After removal of extension, the signal is converted back to standard OFDM signal, followed by serial to parallel conversion. While the effect of channel transforms into a periodic convolution of the discrete-time channel with IFFT of data symbols. Performing FFT non received samples converts the cyclic convolution to multiplication.

FFT gets parallel streams of data in the time domain as input. It converts time OFDM signal to the frequency domain. The output from FFT is set as input to the QAM demodulator. Demodulator separates its bit-stream from the carrier and gives parallel bit streams M_0, M_1, … M_{N-1} as output. These bit-streams are multiplexed using a parallel to serial converter and the outcome of the message signal to be conveyed.

The output from serial to parallel converter is S[n], which is given as an OFDM system.

2.3. Low-density parity-check encoder (LDPC):

A Low-density parity-check (LDPC) code is a linear error-correcting code in Information Theory. In this method, a message is transmitted over a noisy transmission channel. An LDPC is constructed using a sparse Tanner graph (a subclass of the bipartite graph). LDPC codes are capacity-approaching codes, which means that practical constructions exist that allow the noise threshold to be set very close (or even arbitrarily close on the binary erasure channel) to the theoretical maximum (the Shannon limit) for an asymmetric memory-less channel. The noise threshold defines an upper bound for the channel noise, up to which the probability of lost information can be made as small as desired. LDPC codes are decoded in time linear to their block length by using iterative belief propagation techniques.

LDPC codes are characterized by the sparseness of ones in the parity-check matrix. This low number of ones allows for a significant distance of the code, resulting in improved performance. LDPC codes are classified into two different classes of codes – regular and irregular codes. Regular codes are the set of codes in which there is a constant number of $w_{c\ 1}$'s

distributed throughout each column and a constant number of W_R per row. For a determined column weight (w_c), we can determine the row weight as (N+w_c)/(N-k), where N is the block-length of the code, and k is the message length. Irregular codes are those of which do not belong to this set (do not maintain a consistent row weight). The minimum distance is a property of any coding scheme. Ideally, this minimum distance should be as large as possible, but there is a practical limit on how large this minimum distance can be. LDPC poses a large problem when calculating this minimum distance efficiently as effectively as a valid LDPC code requires rather extensive block lengths. Using random generation, it is tough to specify the minimum range as a parameter; instead, minimum distance will become the property of the code.

Using the Tanner graph, it is possible to view the definition of the minimum cycle length of a code. It is the minimum number of edges travelled from one check node to return to the same check node. Length 4 and length six cycles with the corresponding parity-check matrix configurations are shown below

It has been shown that the existence of these cycles degrades the performance during the iterative decoding process. Therefore, when generating the parity check matrix, the minimum cycle length permitted must be determined. It is possible to control the minimum cycle length when making the model; however, computational complexity and time increases exponentially with each increase in minimum cycle length.

LDPC codes are of greater importance and use in applications that require reliable and highly efficient information transfer of information over bandwidth-constrained or return-channel-constrained links in the presence of corrupting noise. Implementation of LDPC codes has always lagged behind other codes, notably turbo codes, till the fundamental patent for Turbo Codes expired on August 29, 2013.

Robert G. Gallager developed the LDPC concept in his doctoral dissertation at the Massachusetts Institute of Technology in 1960. Thereby LDPC codes are also known as Gallager codes in his honour.

2.4. BCH Encoder

In coding theory, the BCH codes or Bose–Chaudhuri–Hocquenghem codes form a class of cyclic error-correcting codes. These BCH codes are constructed using polynomials over a finite field, also called the Galois field. French mathematician Alexis Hocquenghem invented BCH codes in 1959. Raj Bose and D. K. Ray-Chaudhuri invented BCH codes independently in 1960. Thus the name Bose–Chaudhuri–Hocquenghem (and the acronym BCH) arises from the initials of the inventors' surnames (mistakenly, in the case of Ray-Chaudhuri).

One of the key features of BCH codes is that there is precise control over the number of symbol errors correctable by the code during code design. In particular, the binary BCH codes are designed to correct multiple bit errors. Another advantage of BCH code is the ease with which they can be decoded, namely, via an algebraic method known as syndrome decoding. This simplifies the design of the decoder for these codes, using small, low-power electronic hardware.

Satellite communications, compact disc players, DVDs, disk drives, solid-state drives, and two-dimensional bar codes are significant applications of BCH codes.

This class of codes is a remarkable generalization of the Hamming code for multiple-error correction.

For any positive integers $m \geq 3$ and $t < 2m-1$, there exists a binary BCH code with the following parameters:

Block length: $n = 2m - 1$

Number of parity-check digits: $n - k \leq mt$

Minimum distance: $D_{min} \geq 2t + 1$.

We call this code a t-error-correcting BCH code.

2.5 Field of view(FOV)

Field of view (FOV) is the open observable area a person can see through his or her eyes or via an optical device. In the case of optical devices and sensors, FOV describes the angle through which the tools can pick up electromagnetic radiation.

FOV allows for coverage of an area rather than a single focused point. In virtual reality (VR), a large FOV is essential to getting an immersive, life-like experience. Wider FOV also provides better sensor coverage or accessibility for many other optical devices.

Our eyes are the natural start of perception of FOV. In human vision, the field of view is composed of two monocular FOVs, which our brains stitch together to form one binocular FOV. Individually, our eyes have a horizontal FOV of about 135 degrees and a vertical FOV of just over 180 degrees. When the monocular fields of view are stitched together, our binocular FOV gives us around 114 degrees of view horizontally and is necessary for depth perception. Our peripheral vision makes up the remaining 60–70 degrees and has only monocular vision because only one eye can see those sections of the visual field. These measurements are based on the FOV during steady fixation of the eyes.

In addition to monocular and binocular differences in our vision, humans also have different fields of view for different colours. Colour saturation and perception are concentrated in the centre of our FOV and becomes more monochromatic on the edges or periphery of our vision.

2.6. Communication Channels

OFDM is invariably used during channel coding, and most of the time, use a frequency or time interleaving. Frequency (sub-carrier) interleaving increases resistance to frequency-selective channel conditions such as fading. However, time interleaving is of little benefit in slowly fading channels, such as for stationary reception, and frequency interleaving offers little to no interest for narrowband channels that suffer from flat-fading. The reason why interleaving is used in OFDM is to attempt to spread the errors out in the bit-stream that is presented to the error correction decoder, because when such decoders are presented with a high concentration of errors, the decoder is unable to correct all the bit errors, and a burst of uncorrected errors occurs.

However, newer systems usually now adopt near-optimal types of error correction codes that use the turbo decoding principle, where the decoder iterates towards the desired solution.

3. TECHNICAL SPECIFICATION

3.1. Mathematical Formulation of an OFDM Signal

After the qualitative description of the system, it is valuable to discuss the mathematical definition of the modulation system. This allows us to see how the signal is generated and how the receiver must operate, and it gives us a tool to understand the effects of imperfections in the transmission channel. As noted above, OFDM transmits a large number of narrowband carriers, closely spaced in the frequency domain. To avoid a large number of modulators and filters at the transmitter and complementary filters and demodulators at the receiver, it is desirable to be able to use modern digital signal processing techniques, such as fast Fourier transform (FFT). Generally, an OFDM signal can be represented as

$$c(t) = \sum_{n=0}^{N-1} S_n(t) \sin(2\pi f_n t) \tag{3}$$

s(t) = symbols mapped to chosen constellation(PSK/QAM etc..,)

f_n = orthogonal frequency

3.2 Design Parameters of OFDM

Following are the fundamental design parameter chosen for OFDM generation

- FFT length
- Number of used subcarriers
- Bandwidth
- Baseband Sampling Frequency
- Symbol Duration
- Subcarrier Spacing
- Guard Interval/Cyclic Prefix
- Guard Band

In this part, we are going to discuss the steps involved in transmitting the OFDM signal. Initially, the binary stream of data, i.e., the information to be conveyed, is given as input to the system. Unlike other modulation techniques using a single carrier for modulation, OFDM system uses several sub-carriers, one for each input bit-stream symbol. To accomplish this input serial stream of data is converted into parallel streams. Consider a serial bit stream of 3 bits, and its parallel conversion is as shown in Fig. 3.1.
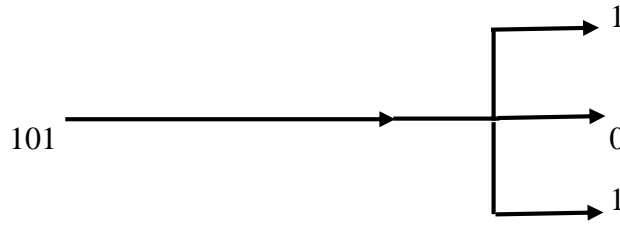
Fig. 3.1 Simple Example Showing Serial to Parallel Conversion

Now, each stream is mapped with a complex symbol stream using QAM. The reason behind choosing these techniques mainly is, they are high-level modulation techniques. Modulation using 4-PSK, 16-PSK, or 4-QAM, 16-QAM helps to increase the data rate of OFDM. A simple illustration of the mechanism going on in this block is given below.
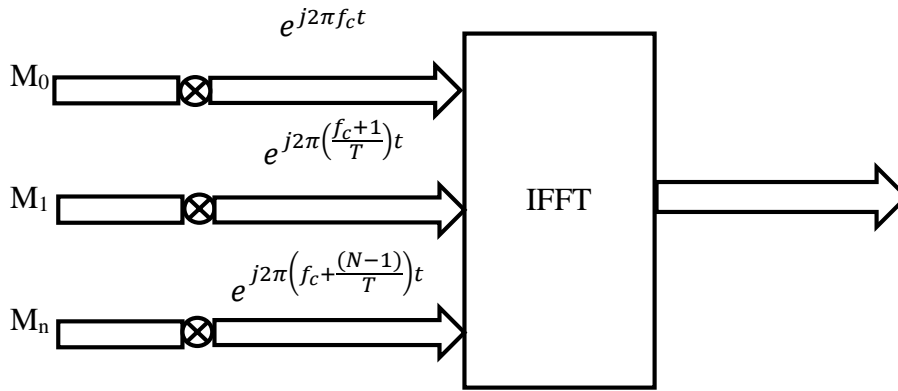

Fig. 3.2 Figure showing Conceptual Modulation Block

In this Fig. 3.2, M_0, M_1, … $M_{(N-1)}$ represents N parallel bit streams obtained after serial to parallel conversion, and each branch corresponds to a sub-carrier. Each sub-carrier modulates a symbol M_K. To maintain orthogonality, the frequency spacing of 1/T Hz is maintained between the successive sub-carriers. This is because sinusoidal signals differing in the frequency 1/T will be orthogonal over the period T.

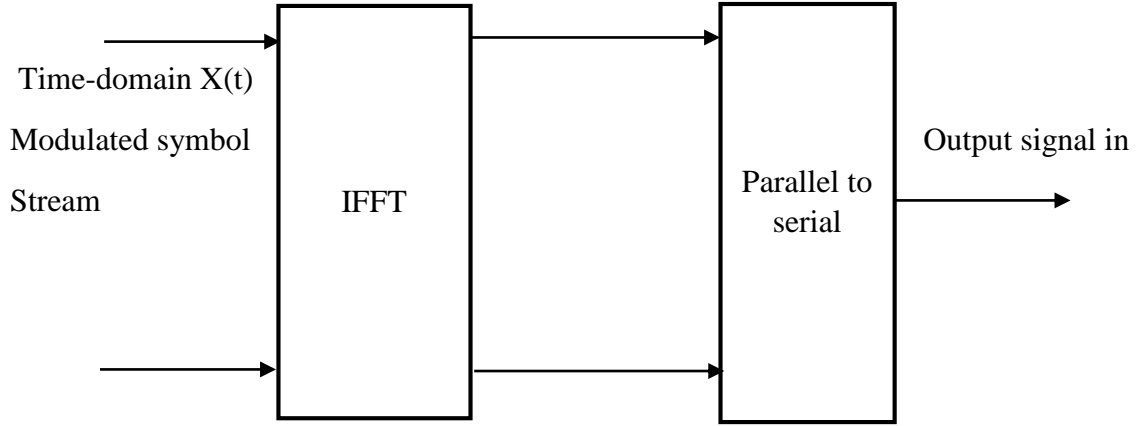$$\int_{tn}^{tn+T} e^{j2\pi f_c t} \left[e^{-j2\pi(f_c+1)/T)t} \right] \mathrm{dt} = 0 \tag{4}$$

Fig. 3.3 IFFT Block Diagram

Individual sub-carriers are arranged, such that the frequency separation between two consecutive sub-carriers is 4f=1/T. If N modulated symbol streams are set as input to IFFT with a symbol duration T, then the output OFDM symbol duration is N*T. The output signal X(t) in the time domain acts as a baseband signal for the OFDM system.

We can define the total bandwidth of an OFDM transmission as:

$$BW= (n+1) \cdot f_0 = (n+1) \cdot 1 \cdot \frac{1}{Ts} \tag{5}$$

Where n is the number of sub-carriers.

3.3. Functions for Impulse Response Modeling

Double Gamma Function

DGFs were first adopted to model the impulse response in the cloud. Inspired by the dispersive nature of both cloud and underwater channels, Tang applied DGFs to model the impulse response in UOWC links. However, such functions are only applicable with relatively large values of the attenuation length.

$$H(t)= C_1 t e^{-C_2 t}+C_3 t e^{-C_4 t} \tag{6}$$

Inspired by the dispersive nature of both cloud and underwater channels, Tang applied DGFs to model the impulse response in UOWC links. However, such functions are only applicable with relatively large values of the attenuation length, where the multiply scattered light is dominant. To generalize these functions, Dong added two parameters to the DGFs and proposed the weighted double gamma functions (WDGF).

Weighted Double Gamma Function (WDGF)

To generalize, these functions, Dong added two parameters to the DGF's and proposed the weighted double gamma functions (WDGF)

$$H(t) = C_1 t^\alpha e^{-C_2 t} + C_3 t^\beta e^{-C_4 t} \tag{7}$$

Where α and β are the two newly added parameters to be determined.

Combination of Exponential and Arbitrary Power Function(CEAPF)

However, after the monte Carlo simulation, it shows that the tail of the impulse function should be convex in WDGF Function.

However, WDGF is a strictly concave function. Although a fit can be made to the experimental data, it will continuously underestimate the intensity of the tail because of this difference of convexity.

Motivated by the problem, A new function was proposed that can be written in the form of a Combination of Exponential and Arbitrary Power Function (CEAPF) as below

$$h(t) = C_1' \frac{(b\Delta L)^\alpha}{(b\Delta L + C2')^\beta} \cdot e^{-a/b.b\Delta L} \cdot e^{-a/b.bL} \tag{8}$$

Where $\Delta L = v\Delta t$, $C_1' = (bv)^{\beta-\alpha} C_1$, $C_2' = bvC_2$, a and b are absorption and scattering coefficients respectively, we can compare different water types with the same scattering length., $C_1 > 0$, $C_2 > 0$, $\alpha > -1$, and $\beta > 0$ are the four parameters to be found, and v is the speed of light in water. To ensure that the function tends to 0 when Δt approaches infinity with arbitrary attenuation coefficient α, we also need to apply the constraint $\beta > \alpha$. These parameters can be calculated from Monte Carlo simulation results using the nonlinear least-squares criterion as

$$(C_1, C_2, \alpha, \beta) = \arg\min \left(\int h(t) - h_{mc}(t)]^2 dt \right) \tag{9}$$

Where h(t) is the CEAPF model, and $h_{mc}(t)$ are the results of the Monte Carlo simulations.

The Table 3.1 lists the values of variables for Combination of Exponential and Arbitrary Power Function (CEAPF) equation [1].

Table 3.1. Parameter of CEAPF in Different UOWC Channels

FOV	C_1	C_2	α	β
L = 5.47 m (b(λ)L = 10), on-axis, harbour water				
20°	5.244×10^{-8}	5.015×10^{-2}	-3.681×10^{-2}	3.019
40°	7.937×10^{-7}	2.957×10^{-2}	-3.595×10^{-2}	1.793
180°	1.390	2.331×10^{-2}	-1.966×10^{-2}	1.564
L = 10.93 m (b(λ)L = 20), on-axis, harbour water				
20°	1.677×10^{-6}	0.2730	0.6577	3.169
40°	1.320×10^{-5}	0.6657	0.4871	3.216
180°	9.072×10^{-6}	0.4374	0.4798	2.005
L = 16.40 m (b(λ)L = 30), on-axis, harbour water				
20°	2.168×10^{-6}	0.6994	1.569	3.739
40°	3.207×10^{-5}	1.463	1.514	4.211
180°	2.236×10^{-5}	1.818	1.255	3.039
L = 10.93 m (b(λ)L = 20), off-axis angle=10°, harbour water				
20°	9.653×10^{-6}	0.3661	3.947	7.765
40°	1.900×10^{-4}	0.8292	2.830	7.129
180°	2.800×10^{-5}	0.4760	3.007	5.183
L = 45.45 m (b(λ)L = 10), on-axis, coastal water				
20°	4.888×10^{-7}	0.4169	-3.681×10^{-2}	3.019
40°	5.525×10^{-7}	0.2458	-3.595×10^{-2}	1.793
180°	5.754×10^{-7}	0.1938	-1.966×10^{-2}	1.564

The Table 3.2 lists the values of variables for Weighted Double Gamma Function(WDGF) [1].

Table 3.2. Parameters of WDGF in Different UOWC Channels

FOV	C_1	C_2	C_3	C_4	α	β
L = 5.47 m (b(λ)L = 10), on-axis, harbour water						
20°	3.67×10^{-5}	57.9	1.44×10^{-5}	17.5	-8.32×10^{-2}	3.21×10^{-2}
40°	3.09×10^{-5}	64.7	2.13×10^{-5}	15.7	-8.68×10^{-2}	3.88×10^{-3}
180°	3.17×10^{-5}	63.8	2.03×10^{-5}	13.8	-8.50×10^{-2}	3.89×10^{-3}
L = 10.93 m (b(λ)L = 20), on-axis, harbour water						
20°	9.41×10^{-7}	8.68	1.49×10^{-7}	2.38	0.556	0.444
40°	6.06×10^{-7}	5.37	2.23×10^{-7}	1.67	0.474	0.461
180°	5.13×10^{-7}	4.51	2.02×10^{-7}	1.07	0.441	0.413
L = 16.40 m (b(λ)L = 30), on-axis, harbour water						
20°	4.65×10^{-9}	2.45	5.13×10^{-10}	0.640	1.12	0.673
40°	6.44×10^{-9}	1.77	9.84×10^{-10}	0.575	1.24	0.890
180°	4.79×10^{-9}	1.30	1.36×10^{-10}	0.432	1.10	0.998
L = 10.93 m (b(λ)L = 20), off-axis angle=10°, harbour water						
20°	4.36×10^{-6}	6.38	9.52×10^{-8}	2.35	2.46	1.84
40°	2.33×10^{-6}	4.73	1.65×10^{-7}	2.00	2.24	1.99
180°	1.84×10^{-6}	4.34	1.69×10^{-7}	1.49	2.17	1.82
L = 45.45 m (b(λ)L = 10), on-axis, coastal water						
20°	1.37×10^{-9}	7.00	4.22×10^{-10}	2.13	-8.32×10^{-2}	3.21×10^{-2}
40°	1.16×10^{-9}	7.82	6.61×10^{-10}	1.92	-8.68×10^{-2}	3.88×10^{-3}
180°	1.19×10^{-9}	7.70	6.31×10^{-10}	1.69	-8.50×10^{-2}	3.89×10^{-3}

4. DESIGN APPROACH AND DETAILS

4.1 Design Parameters

 We have listed different parameters in Table 4.1 all the parameters that we have used to design this experiment

Table.4.1 Design Parameters

Parameters	Values
Mapping and De-mapping Schemes	4-QAM, 16-QAM, 4-PSK, 16-PSK-OFDM
Modulation type	OFDM
No. of Subcarrier	52
No. of Data Bits	32400
Length of Cyclic Prefix	54
Error correction codes	BCH and LDPC encoding
Impulse response model	CEAPF model
Channel type	Harbour water and Coastal water
Absorption coefficient	$a=0.179m^{-1}$ (Coastal water) $a=0.366m^{-1}$ (Harbour water)
Scattering coefficient	$b=0.220m^{-1}$(Coastal water) $b=1.829m^{-1}$ (Harbour water)
Speed of light	$2.237*10^8 ms^{-1}$

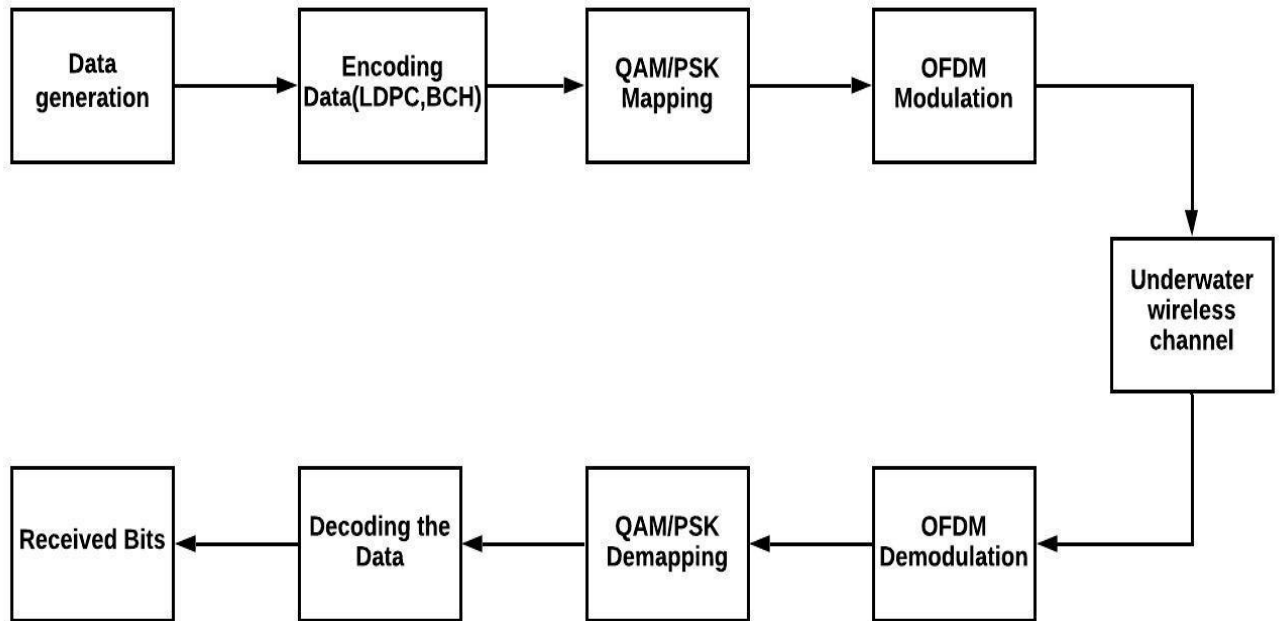**4.2** General Block Diagram of LDPC/BCH Encoded OFDM**:**

Fig. 4.1 General Block Diagram of LDPC/BCH Encoded OFDM

This project's design is given in Fig4.1, which can be divided into three parts, i.e., transmitter, receiver, and channel. We will see the function of each component in the subsequent sections. Initially, we start with the generation of data; the no. The data points we used for this experiment is 32400 bits. For generating the data points, we randomly assign 0's and 1's up to 32400 bits. After the data generation, we then encode the data using error correction techniques like LDPC and BCH encoding. After the Encoding, the data points are doubled and tripled for LDPC and BCH encoding, respectively. Next, we move to map schemes of the encoded data to 4-QAM, 16-QAM, 4- PSK, 16-PSK. After the mapping of data points. We feed it into Orthogonal frequency division multiplexing (OFDM) modulator.

In the next step, we simulate an Underwater wireless channel using the CEAPF impulse function [1]. This CEAPF impulse model [1] is a function of three real-world parameters that affect the channel performance, and they are absorption coefficient, scattering coefficient, and the length of the channel. Then we transmit this OFDM signal into the simulated underwater wireless channel. For this purpose, we convolve two functions, i.e., channel impulse function and the generated OFDM function. We use two types of the underwater wireless channel for this experiment, and the first one is the harbour water wireless channel and the coastal water wireless channel. We can see that the difference between these two water types is that they mainly differ in their absorption and scattering coefficients. The coastal water has relatively low absorption and scattering coefficients compared to the harbour water. Once the convolution takes place, we move into the receiver.

In the receiver, we first demodulate the received OFDM signal after the convolution with the channel. Then we can apply the QAM/PSK de-mapping to the demodulated signal.

24

After the de-mapping, we will decode the data which initially encoded in the transmitter using BCH or LDPC encoder. After the signal decoding, we move to find the Bit error rate of the received signal. For this purpose, we compare every bit received against every bit transmitted. Then we divide the error bits from total bits to arrive at the BER rate. Until this process is just the end of the first cycle, for the next cycle, we increase the length of the channel and repeat the same process until the BER is maximum, and the received signal is no longer able to reach this length. With this cycle, by increasing the length of the signal after each iteration, we can find the maximum length of a signal to travel on a particular channel.

We simulate all the processes mentioned above for a different combination of error correction encoding techniques (i.e., LDPC or BCH) and different mapping schemes (i.e., 4-QAM, 16-QAM, 4-PSK, 16-PSK) and various water types. At the end of this experiment, we can find out Which Error correction code with a combination of mapping schemes can be used to provide the best bit error rate(BER) for the Different Underwater wireless channel.

4.3 Codes and Standards

In this project, we use MATLAB R2017a for all the simulations that are being executed. For this purpose, we use a Communication toolbox that is available in the MATLAB for Encoding and decoding the signal; the rest of the process does not require any additional toolboxes from MATLAB. IEEE **802.11a** is the standard we use to generate OFDM signal

4.4 Constraints, Alternatives and Tradeoffs

The primary constraint of this project is that even though the real-time water channel impulse function is affected by absorption, scattering, turbulence-induced fading caused by temperature and salinity of water, as well as randomly distributed air bubbles in the water. However, to reduce the complexity of the analysis, we have only taken the effects of absorption and scattering, the properties of which can be described by the inherent optical properties (IOPs) of the water.

This project's channel impulse function is based on our base paper [1], which offers only two different types of channels, i.e., harbour water and coastal water. It is because this CEAPF channel model is newly proposed. Moreover, we do not have enough data to simulate channel for other water types, other than the types mentioned above. Thus, our project is limited to only these two water types. Furthermore, the base paper provides equation constraints only for three different Fields of views (FOV) (i.e., FOV=180,40,20). Thus, this project contains results only to these three different FOV's.

In this underwater wireless channel, we have experimented with 4-QAM, 16-QAM, 4-PSK, 16-PSK. We were limited to modulation order of 16 because, when we increase the modulation order, the data rate increases; thus, the signal attenuates massively even for short link lengths. Moreover, we were not able to receive the total message signal

transmitted above the modulation order of 16. So, it is evident that when we move to a higher modulation order, the Spectral efficiency of the system is affected severely.

When we see the BER vs Length output graph of the PSK modulation, we can observe that the plot suddenly stops after reaching its peak, unlike QAM modulation, where the plot continues even after reaching the summit. This behavior is only seen in PSK because, after a certain length, only half of the transmitted signal is received. Since this graph is a computer-generated, we cannot decode the message when only half of the signal is received. So, after a certain length, we stop simulation manually to avoid the error.

5. SCHEDULE TASKS AND MILESTONE

Table 5.1 describes the time deadline and work completion.

Table 5.1 Schedule of Project

Deadline	Tasks
2nd DEC - 22nd DEC	Working on the literature review of the project
23rd DEC - 14th JAN	Title discussion and the paper selection and literary survey.
15th JAN – 31st JAN	I started learning about the MATLAB and kept working on the literature review.
1st FEB – 20th FEB	Design of Channel Modelling
21st FEB – 4th MAR	Design of transmitter with QAM/PSK mapping with OFDM .
5th MAR – 20th MAR	Transmitting QAM, PSK, signals through the channel model and Designing the receiver
21st MAR – 4th APR	Generating and analyzing the output results and the bit error rate.
5th APR – 21st APR	Encoding the signal with LDPC and BCH error correction codes at the transmitter
22nd APR – 4th MAY	Transmitting the encoded signal through a model channel.
5th MAY – 11th MAY	Analyzing the results of 4QAM, 4-PSK, 16-QAM, 16-PSK OFDM with Encoding, and without Encoding.
12th MAY – 27th MAY	The final report thesis is completed with the required format. Manuscript for paper is prepared and poster of the project is designed.

6. PROJECT DEMONSTRATION

In this part of the section, we are going to display all the results that we have generated in this project.

Initially, we will see the channel Impulse response that we have generated from the CEAPF channel model [1] for coastal and harbour water. In the next section, we will display all the BER vs Length graph we generated with different combinations of mapping schemes and error correction techniques.

6.1 Simulated Results for channel Impulse function combination of exponential and arbitrary power function(CEAPF)[1]:

.
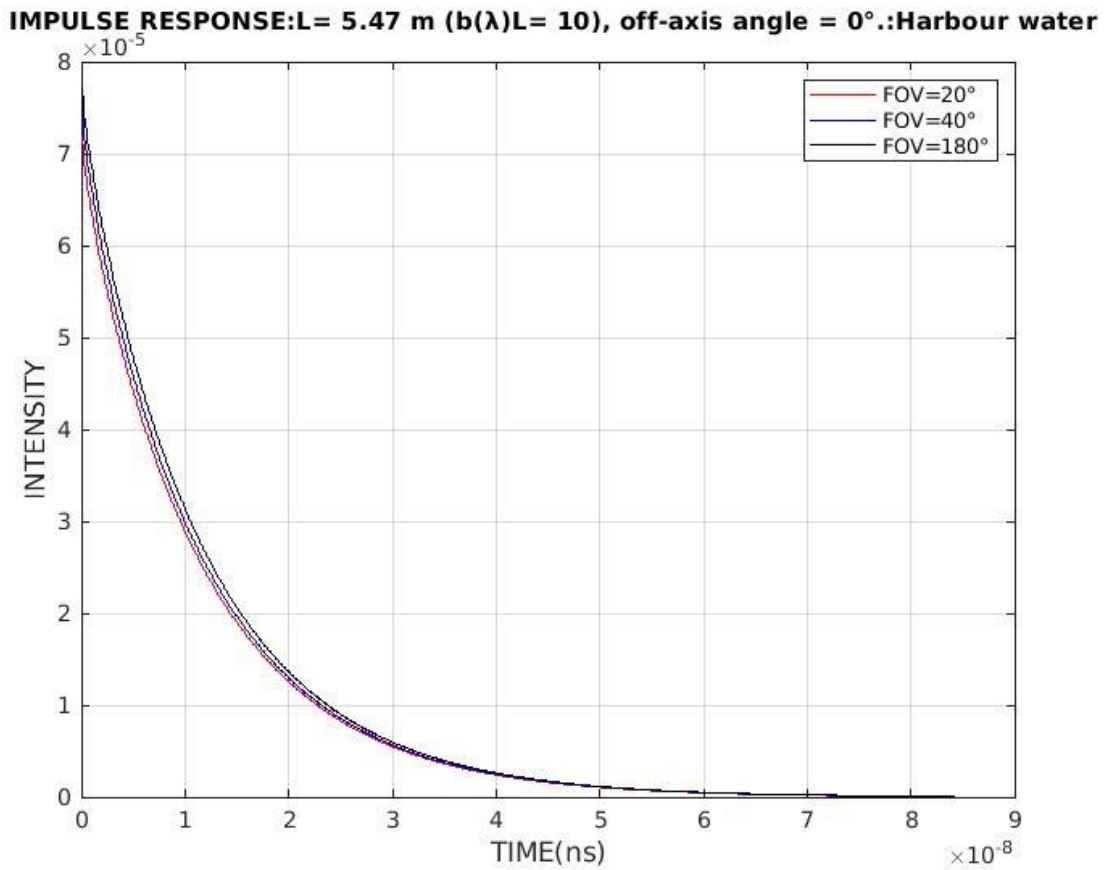
Fig. 6.1 Simulation result for channel impulse L=5.47m unit

The Fig 6.1 Shows the impulse response for Harbour water for a channel length of 5.47 m for three Field Of Views $=20^0,40^0,180^0$. We can see that the peak is highest for FOV$=180^0$. The intensity is in the order of 10^{-5}.
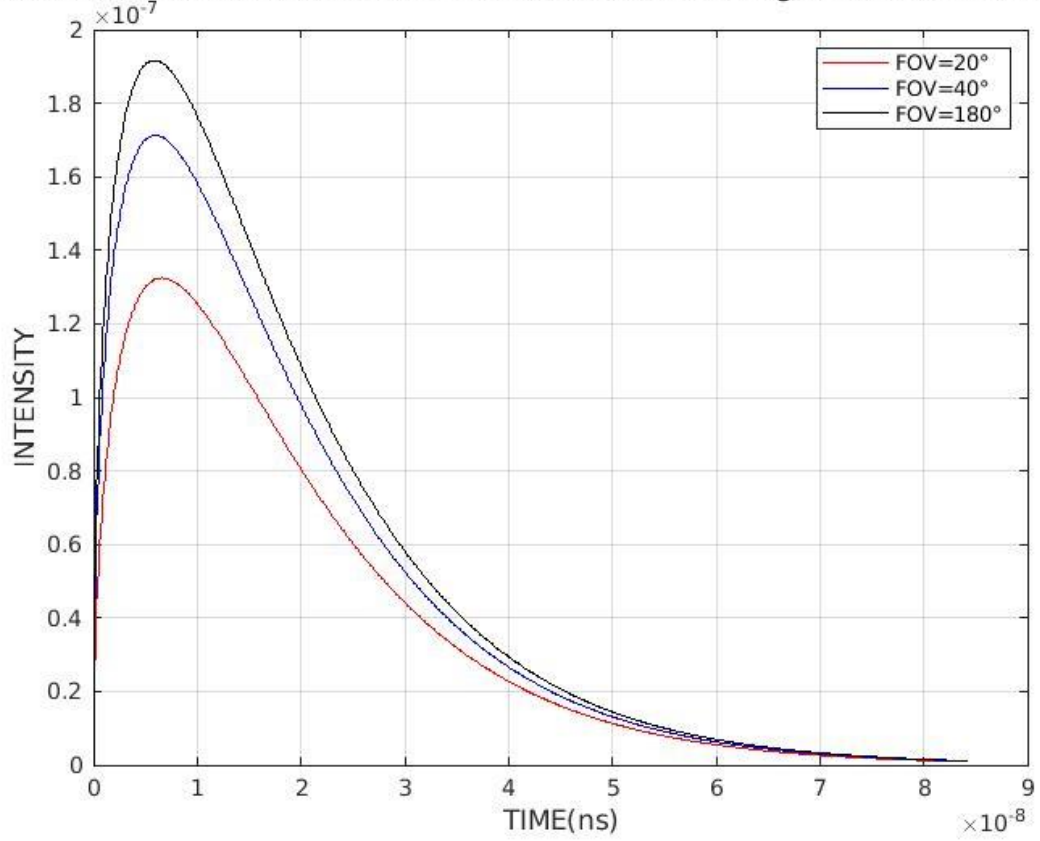
Fig. 6.2 Simulation result for channel impulse L=10.93m
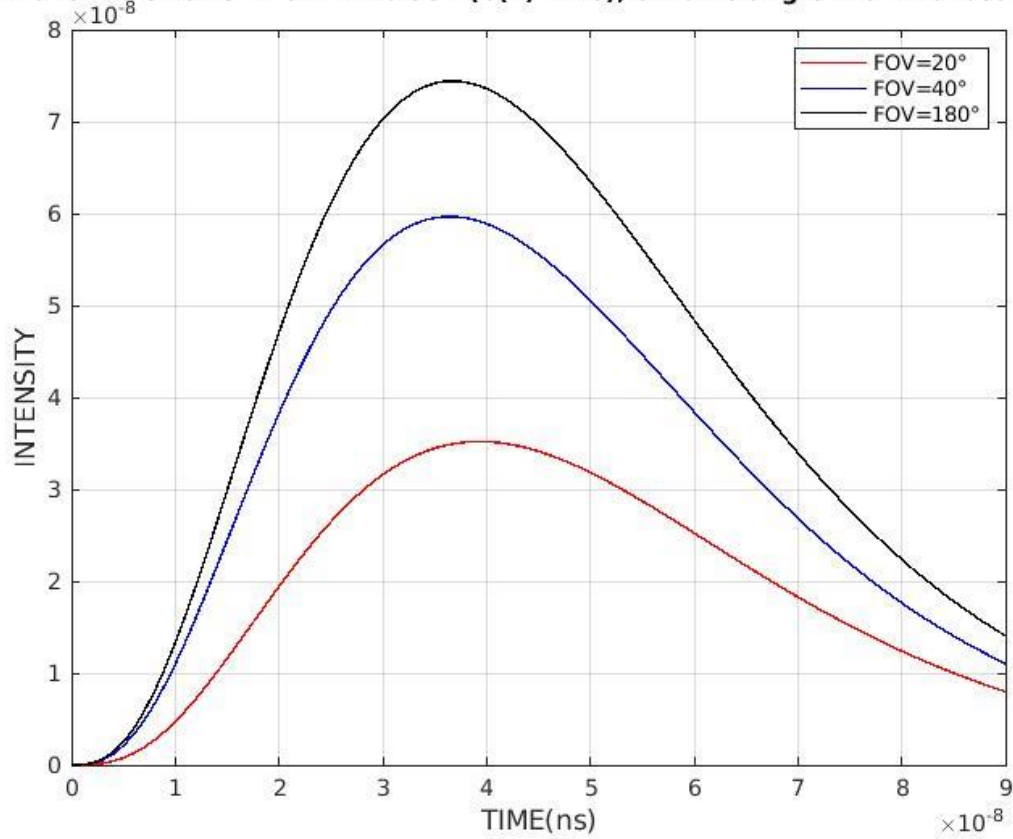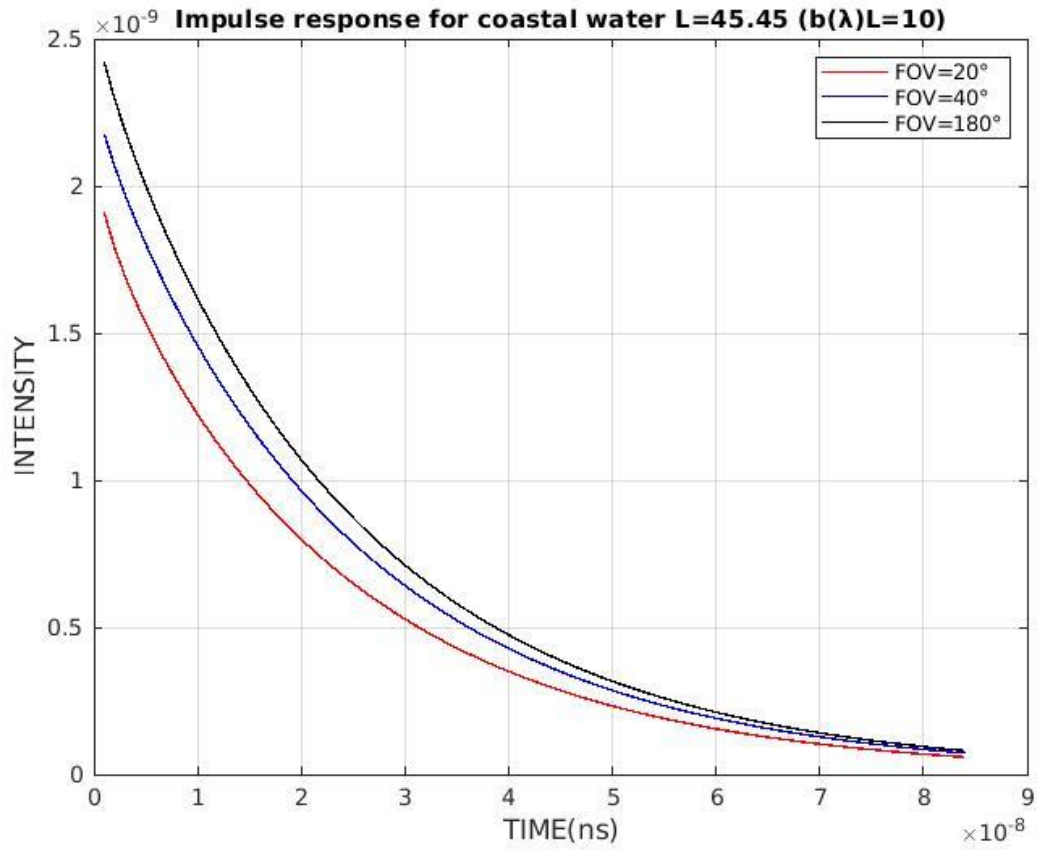
The Fig 6.2 Shows the impulse response for Harbour water for a channel length of 10.93m for three Field of Views =20^0,40^0,180^0. We can see that the peak is highest for FOV=180^0. The intensity is in the order of 10^{-7}. Comparing Fig 6.2 to Fig 6.1 we can notice that the peak of the Impulse Response is slightly shifted right and also the peak values is down by an order of 2.
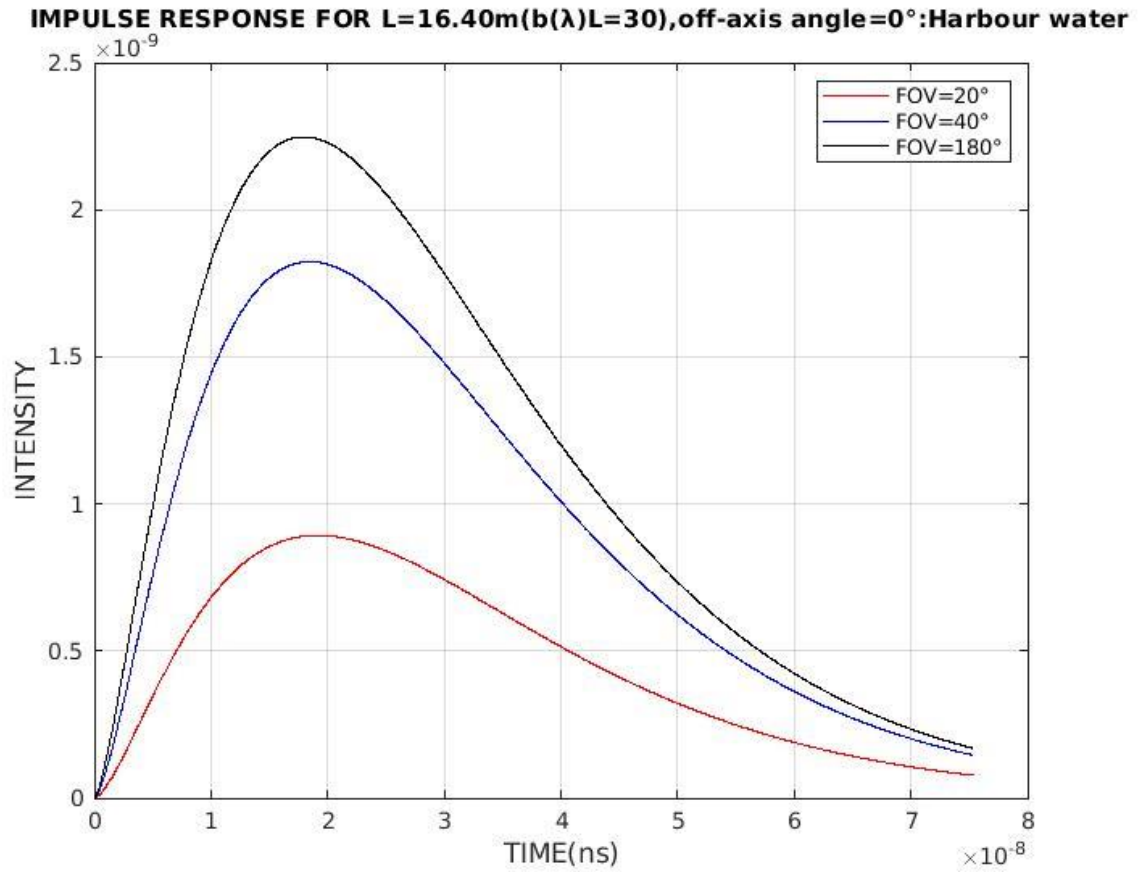
Fig. 6.3 Simulation result for channel impulse L=16.40m

The Fig 6.3 Shows the impulse response for Harbour water for a channel length of 16.40m for three Field of Views $=20^0,40^0,180^0$. We can see that the peak is highest for FOV$=180^0$. The intensity is in the order of 10^{-9}. Comparing Fig 6.3 to Fig 6.2 we can notice that the peak of the Impulse Response is slightly shifted right and also the peak value is decreased by an order of 2.

Fig. 6.4 Simulation result for channel impulse L=10.93m for angle=10°

The Fig 6.4 Shows the impulse response for Harbour water for a channel length of 10.93m for three Field of Views =$20^0,40^0,180^0$ for an off axis angle of 10^0 . We can see that the peak is highest for FOV=180^0. The intensity is in the order of 10^{-8}. Comparing Fig 6.4 to Fig 6.3 we can notice that the peak of the Impulse Response is slightly shifted right and also the peak values is incresed by an order of 1.

Fig. 6.5 Simulation result for channel impulse coastal water L=45.45m

The Fig 6.5 Shows the impulse response for Coastal water for a channel length of 45.45 m for three Field of Views $=20^0,40^0,180^0$. We can see that the peak is highest for FOV=180^0. The intensity is in the order of 10^{-9}.

6.2 Bit error rate (BER) and length Performance analysis of simulated CEAPF channel:
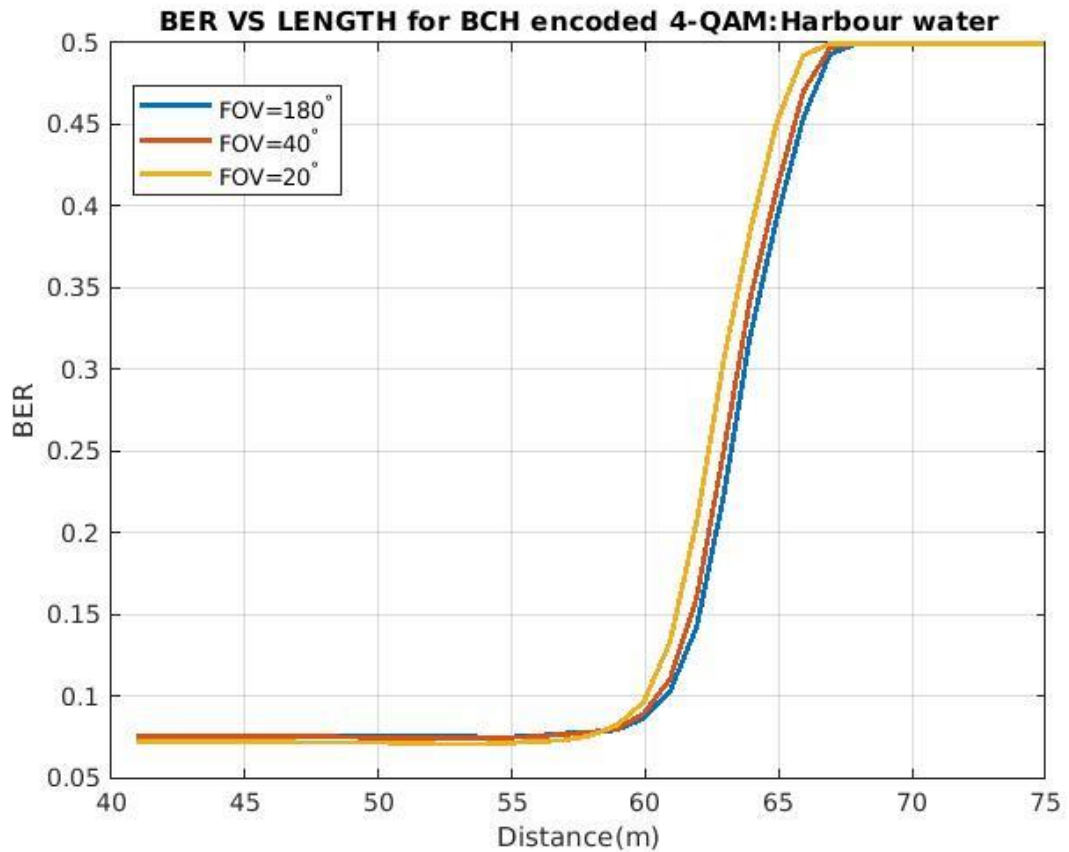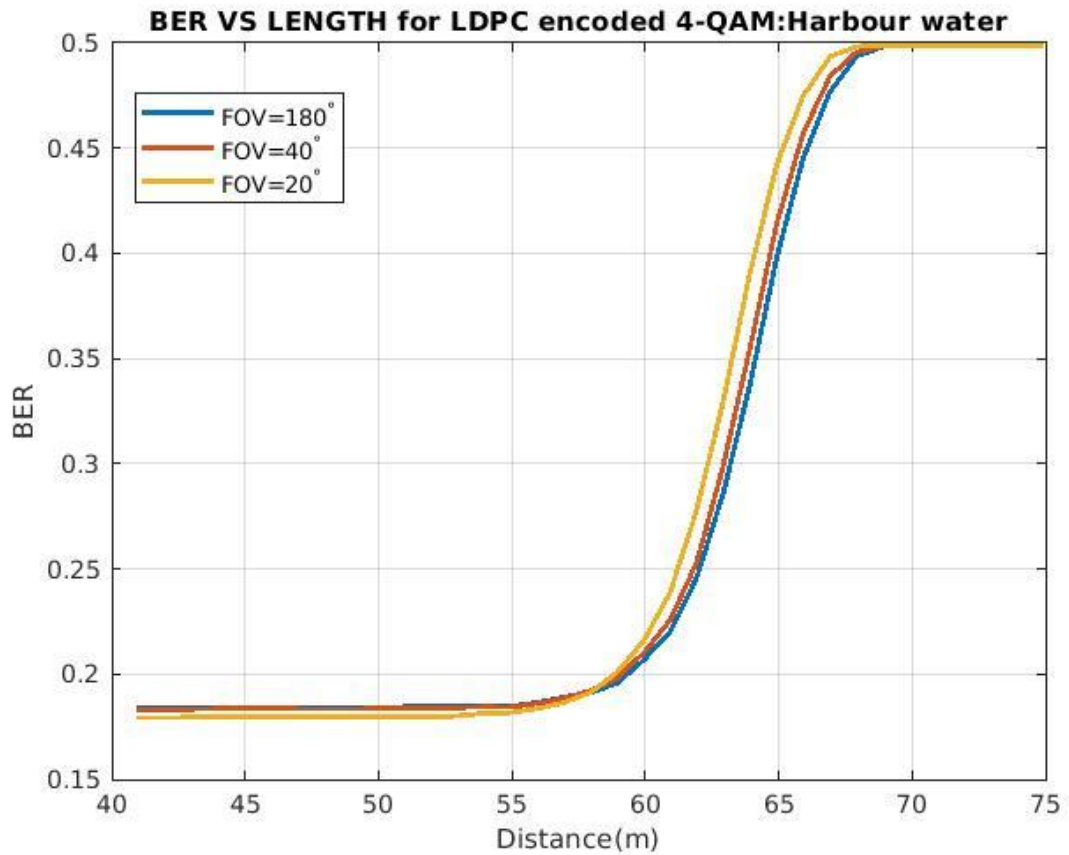
6.2.1. 4-QAM-OFDM IN HARBOUR WATER

Fig. 6.6 BER VS LENGTH FOR 4-QAM BCH Encoding for Harbour water

In this case, a fourth-order QAM-OFDM modulation technique of order four is used with the BCH encoding technique. The bit error rate is 0.0717, with a maximum distance of 62m.We can see that out of three different Field Of View , the transmitting length is maximum for FOV $=180^0$.
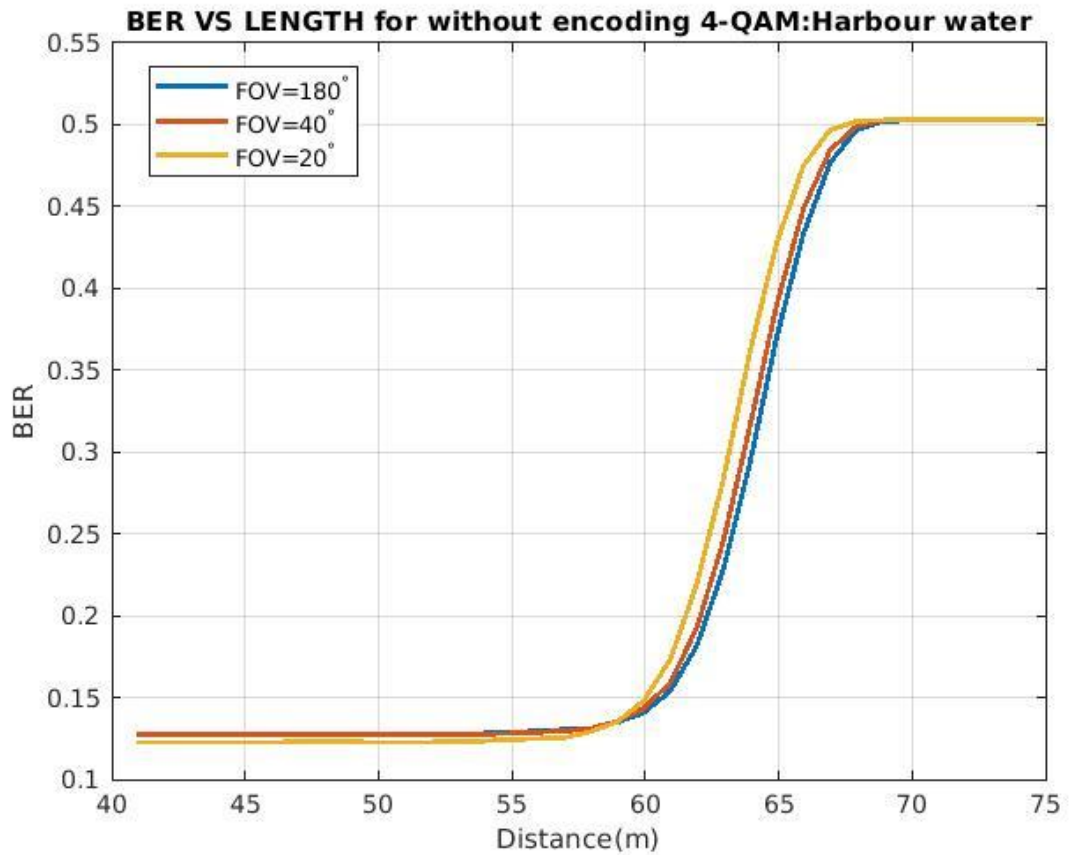
6.2.2. 4-QAM-OFDM IN HARBOUR WATER

Fig. 6.7 BER VS LENGTH For 4-QAM LDPC Encoding for Harbour water

In this case, QAM-OFDM modulation of order four is used with the LDPC encoding technique. The bit error rate is 0.1739, with a maximum distance of 62m. We can see that out of three different Field Of View the transmitting length is maximum for FOV $=180^0$.

6.2.3. 4-QAM-OFDM IN HARBOUR WATER

BER VS LENGTH for without encoding 4-QAM:Harbour water

Fig 6.8 BER VS LENGTH For 4-QAM without Encoding for Harbour water

In this case, QAM-OFDM modulation of order four is used without any encoding technique. The bit error rate is 0.1343, with a maximum distance of 62m. We can see that out of three different Field Of View the transmitting length is maximum for FOV $=180^0$. When we Compare Fig 6.8 ,Fig 6.7, and Fig 6.6 we can clearly notice that the BCH encoded signal provides the best BER for 4-QAM signal in the harbour water channel.
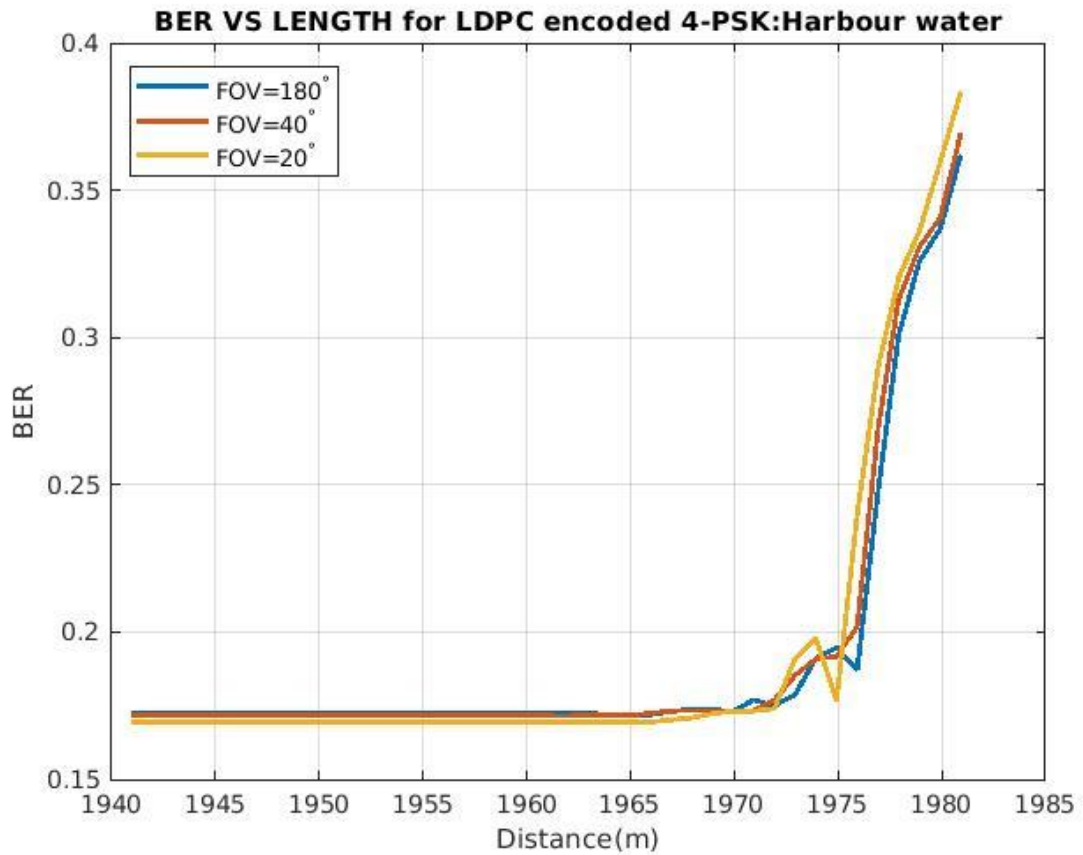
6.2.4. 4-PSK-OFDM IN HARBOUR WATER
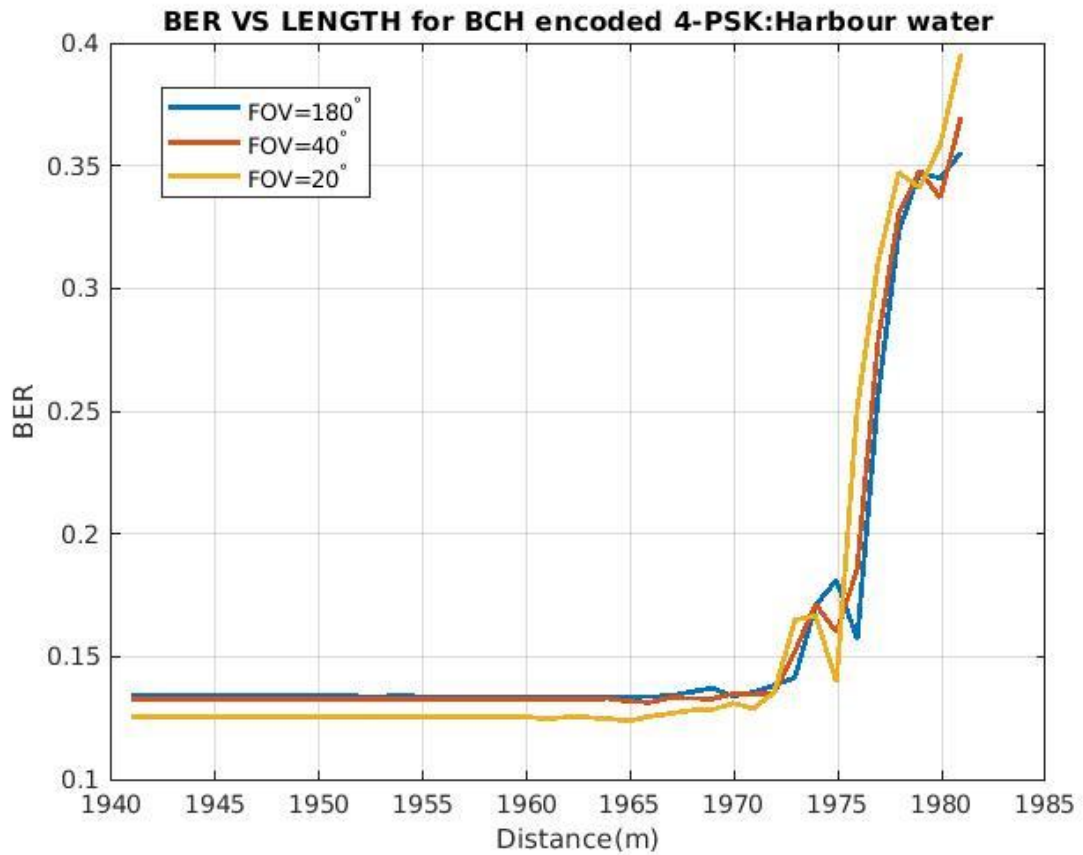
Fig. 6.9 BER VS LENGTH For 4-PSK BCH Encoding for Harbour water

In this case, PSK-OFDM modulation of order four is used with the BCH encoding technique. The bit error rate is 0.1238, with a maximum distance of 1982m. We can see that out of three different Field Of View the transmitting length is maximum for FOV $=180^0$
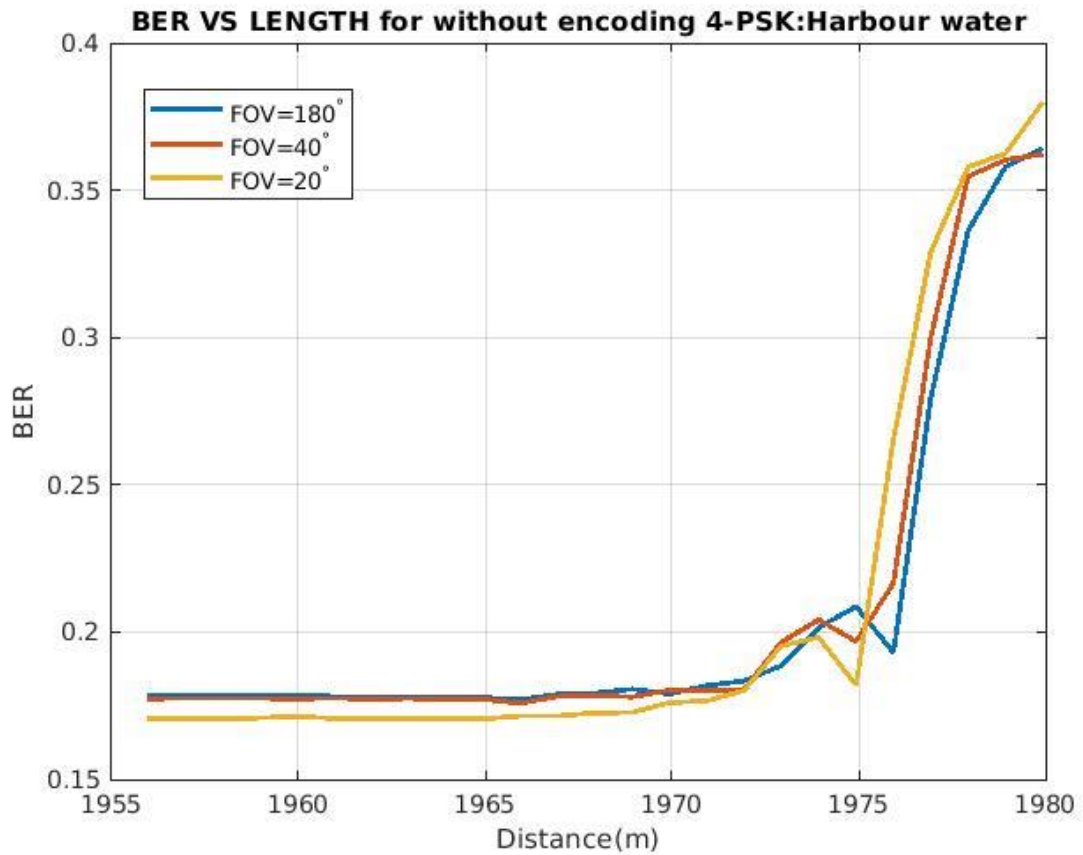
6.2.5. 4-PSK-OFDM IN HARBOUR WATER

Fig. 6.10 BER VS LENGTH For 4-PSK LDPC Encoding for Harbour water

In this case, PSK-OFDM modulation of order four is used with the LDPC encoding technique. The bit error rate is 0.1739, with a maximum distance of 1982m. We can see that out of three different Field Of View the transmitting length is maximum for FOV $=180^0$
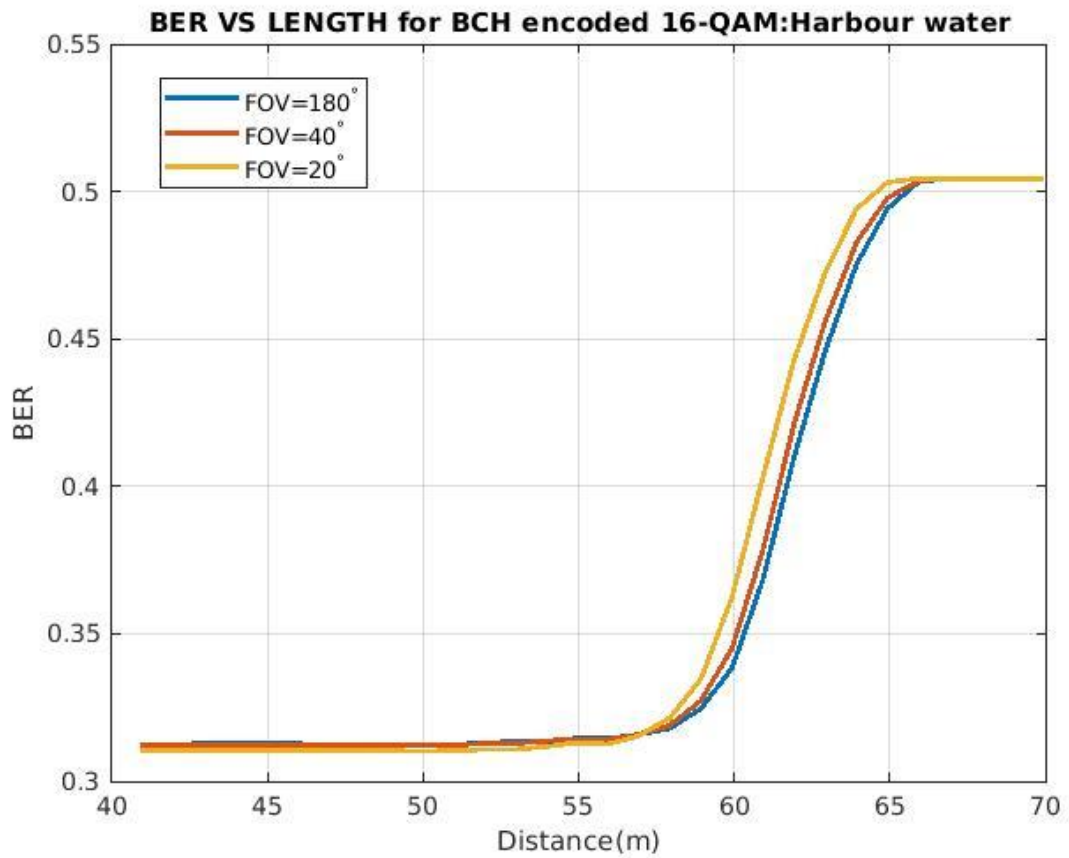
6.2.6. 4-PSK-OFDM IN HARBOUR WATER

Fig. 6.11 BER VS LENGTH For 4-PSK without Encoding for Harbour water

In this case, PSK-OFDM modulation of order four is used without any encoding technique. The bit error rate is 0.1725, with a maximum distance of 1982m. We can see that out of three different Field Of View the transmitting length is maximum for FOV $=180^0$. When we Compare Fig 6.11, Fig 6.10, and Fig 6.9 we can clearly notice that the BCH encoded signal provides the best BER for 4-PSK signal in the harbour water channel.

6.2.7. 16-QAM-OFDM IN HARBOUR WATER

BER VS LENGTH for BCH encoded 16-QAM:Harbour water

Fig. 6.12 BER VS LENGTH For 16-QAM BCH Encoding for Harbour water

In this case, PSK-OFDM modulation of the order 16 is used with the BCH encoding technique. The bit error rate is 0.307, with a maximum distance of 62m. We can see that out of three different Field Of View the transmitting length is maximum for FOV $=180^0$
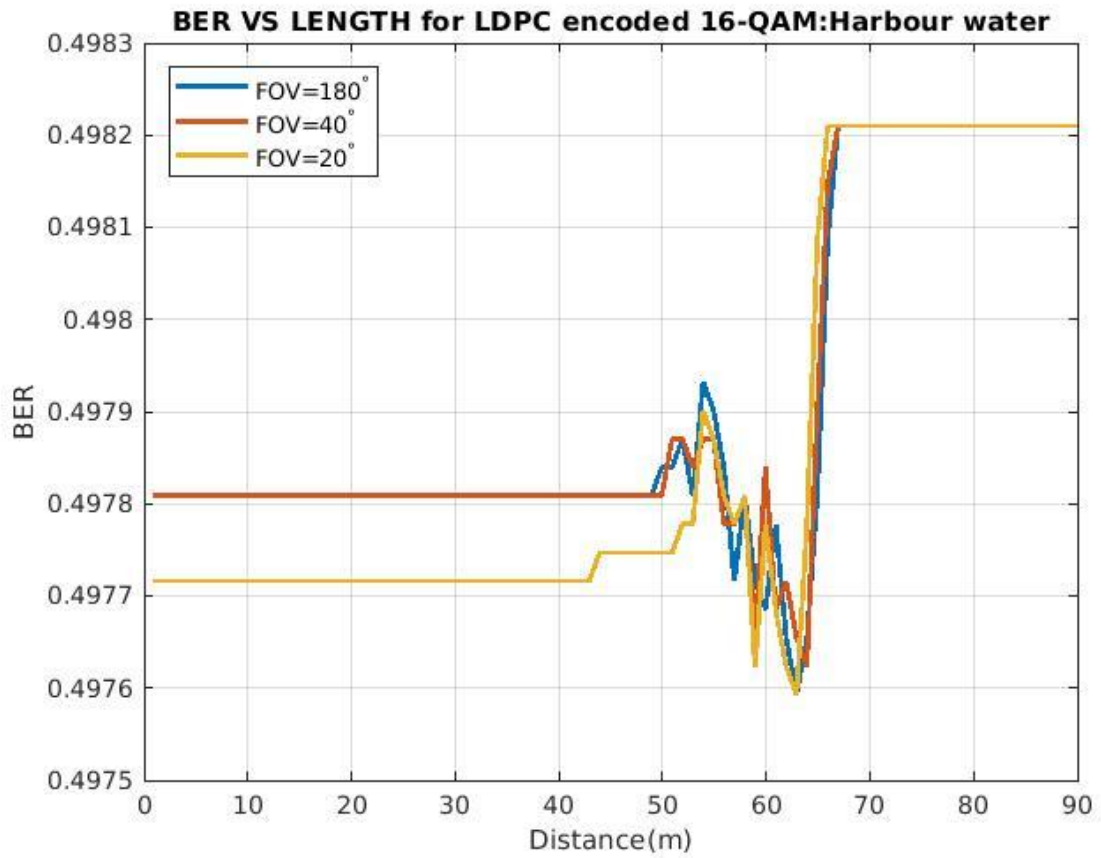
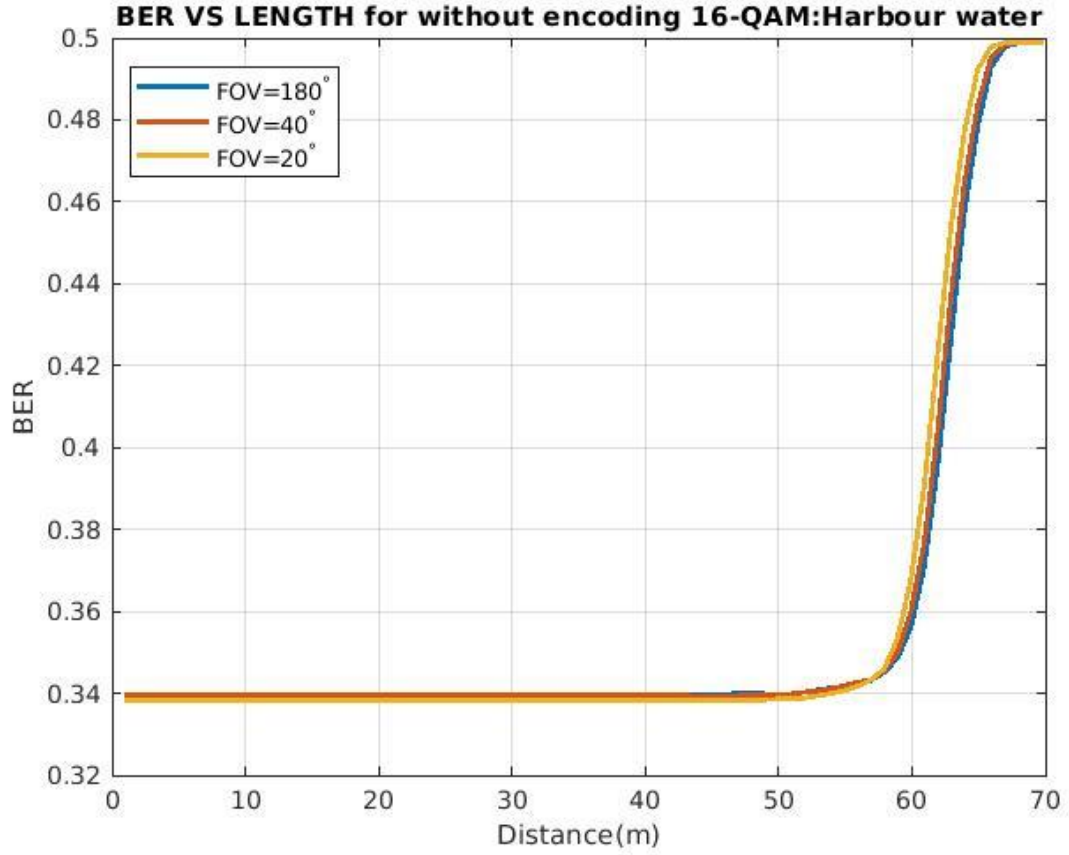## 6.2.8. 16-QAM-OFDM IN HARBOUR WATER

Fig. 6.13 BER VS LENGTH For 16-QAM LDPC Encoding for Harbour water

In this case, QAM-OFDM modulation of the order 16 is used with the LDPC encoding technique. The bit error rate is 0.4919 with a maximum distance of 48m. We can see that out of three different Field Of View the transmitting length is maximum for FOV =180^0
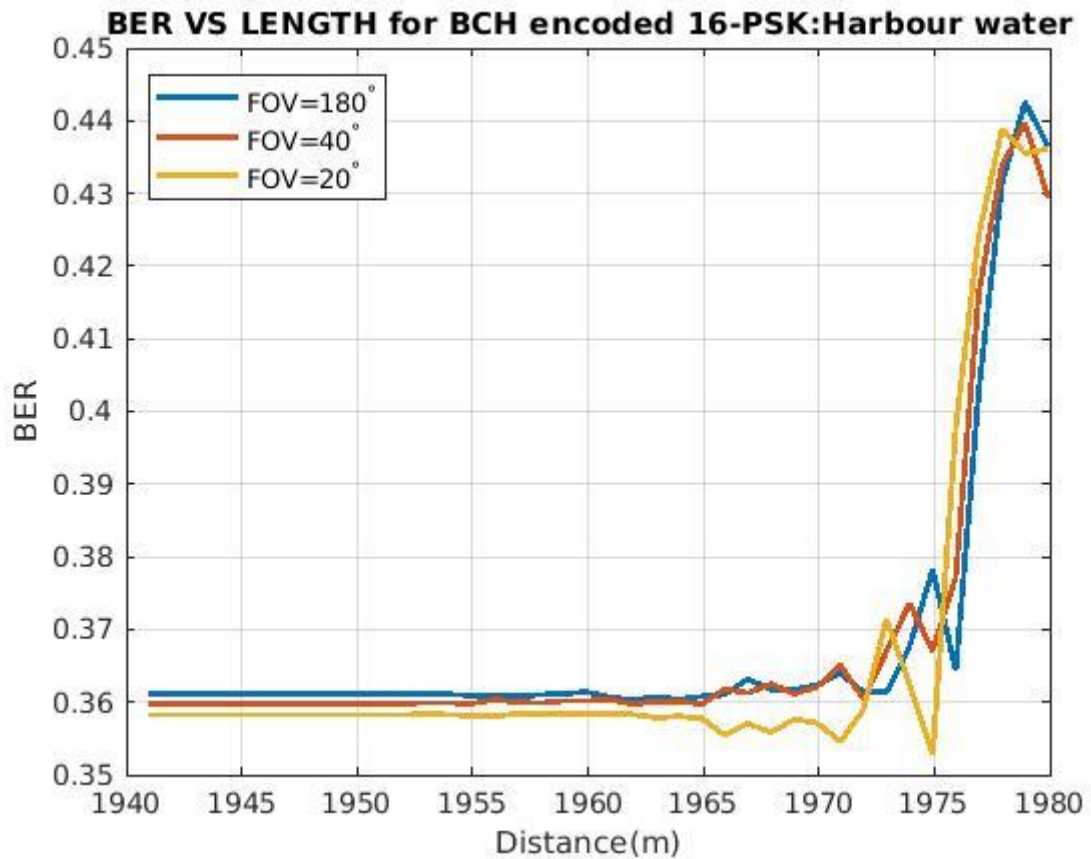
6.2.9. 16-QAM-OFDM IN HARBOUR WATER

Fig. 6.14 BER VS LENGTH For 16-QAM without Encoding for Harbour water

In this case, QAM-OFDM modulation of the order 16 is used without any encoding technique. The bit error rate is 0.3378, with a maximum distance of 62m. We can see that out of three different Field Of View the transmitting length is maximum for FOV $=180^0$. When we Compare Fig 6.14 ,Fig 6.13, and Fig 6.12 we can clearly notice that the BCH encoded signal provides the best BER for 16-QAM signal in the harbour water channel.

6.2.10. 16-PSK-OFDM IN HARBOUR WATER

Fig. 6.15 BER VS LENGTH For 16-PSK BCH Encoding for Harbour water

In this case, PSK-OFDM modulation of the order 16 is used with the BCH encoding technique. The bit error rate is 0.3615, with a maximum distance of 1982m. We can see that out of three different Field Of View the transmitting length is maximum for FOV $=180^0$
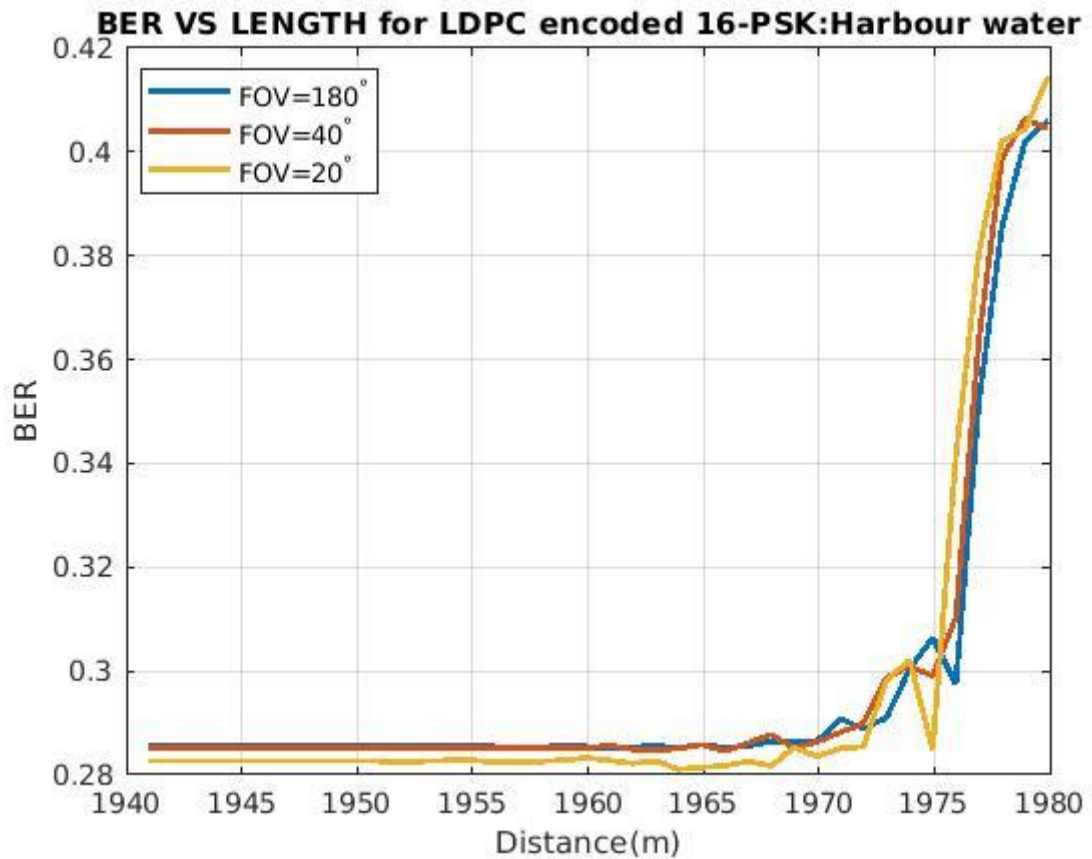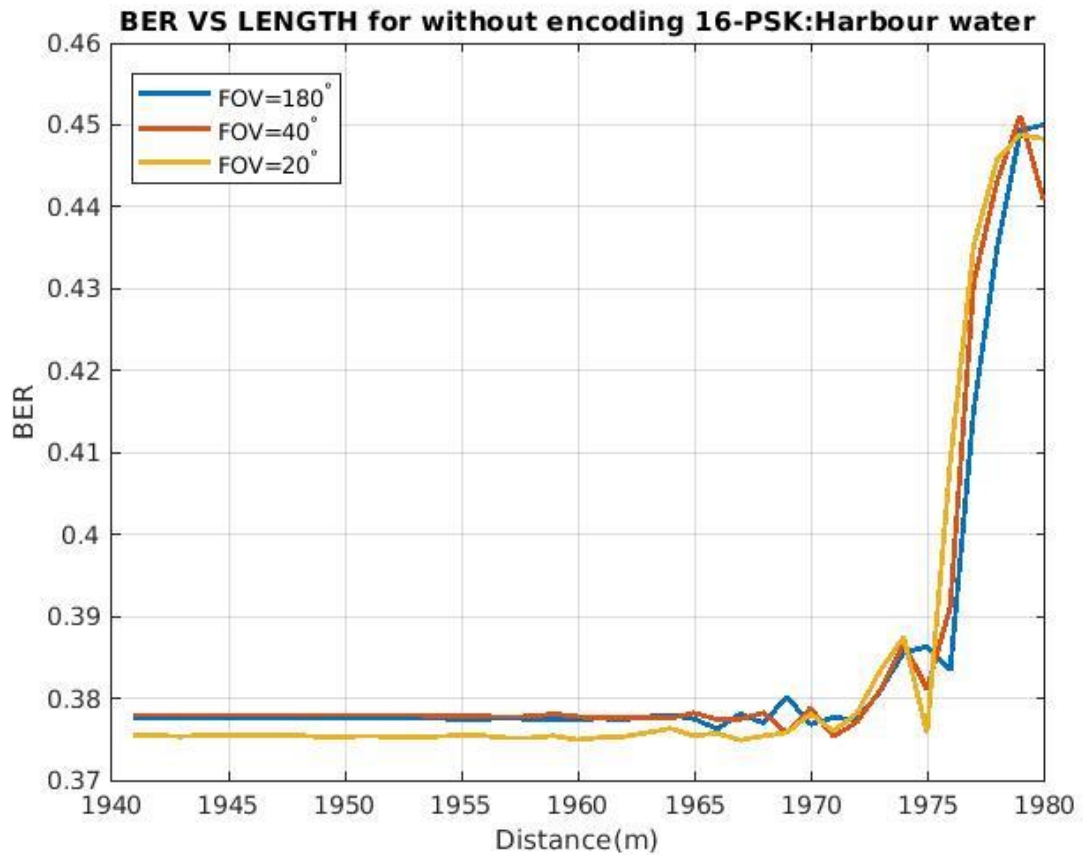
6.2.11. 16-PSK-OFDM IN HARBOUR WATER

Fig. 6.16 BER VS LENGTH For 16-PSK LDPC Encoding for Harbour water

In this case, PSK-OFDM modulation of the order 16 is used with the LDPC encoding technique. The bit error rate is 0.2786, with a maximum distance of 1982m. We can see that out of three different Field Of View the transmitting length is maximum for FOV $=180^0$

6.2.12. 16-PSK-OFDM IN HARBOUR WATER

BER VS LENGTH for without encoding 16-PSK:Harbour water

Fig. 6.17 BER VS LENGTH For 16-PSK without Encoding for Harbour water

In this case, PSK-OFDM modulation of the order 16 is used without any encoding technique. The bit error rate is 0.3753, with a maximum distance of 1982m. We can see that out of three different Field Of View the transmitting length is maximum for FOV $=180^0$. When we Compare Fig 6.17, Fig 6.16, and Fig 6.15 we can clearly notice that the BCH encoded signal provides the best BER for 16-PSK signal in the harbour water channel.

6.2.13. 4-QAM-OFDM IN COASTAL WATER

Fig. 6.18 BER VS LENGTH For 4-QAM BCH Encoding for Coastal water

In this case, QAM-OFDM modulation of order four is used with the BCH encoding technique. The bit error rate is 0.0525, with a maximum distance of 161.9m. We can see that out of three different Field Of View the transmitting length is maximum for FOV $=180^0$.
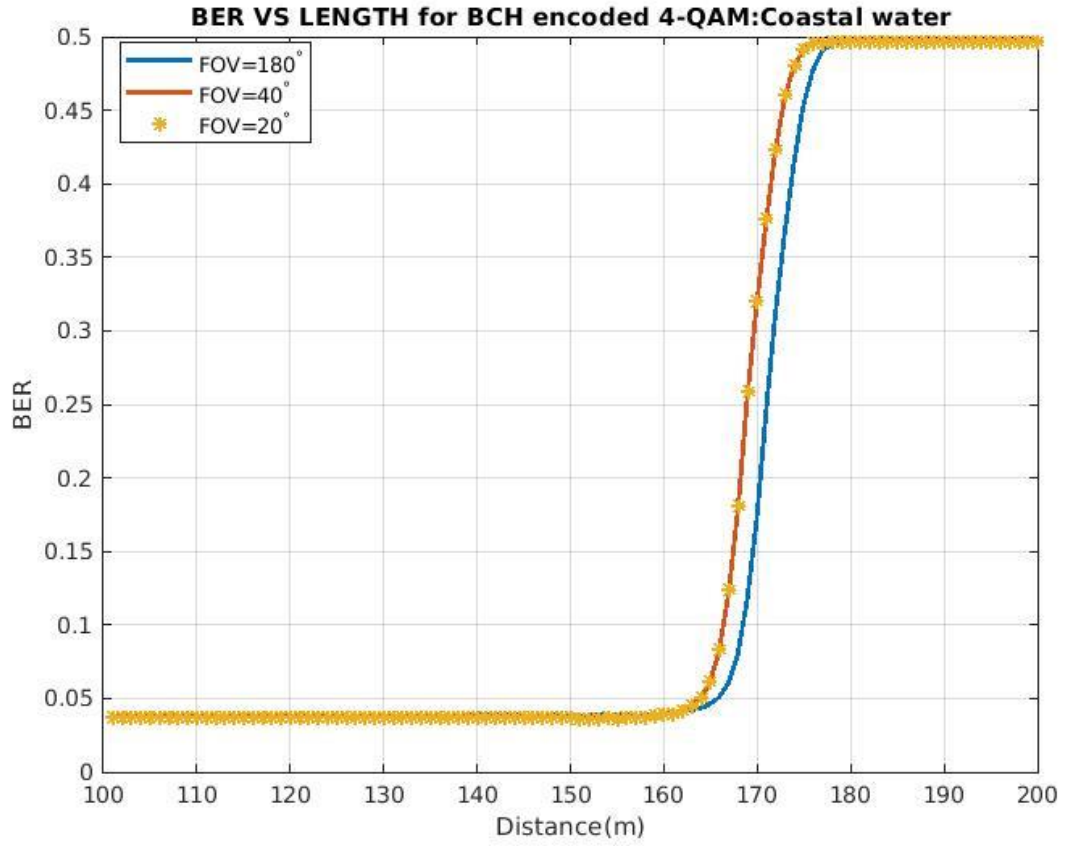
6.2.14. 4-QAM-OFDM IN COASTAL WATER

Fig. 6.19 BER VS LENGTH For 4-QAM LDPC Encoding for Coastal water

In this case, QAM-OFDM modulation of order four is used with the LDPC encoding technique. The bit error rate is 0.1260 with a maximum distance of 161.9. We can see that out of three different Field Of View the transmitting length is maximum for FOV $=180^0$
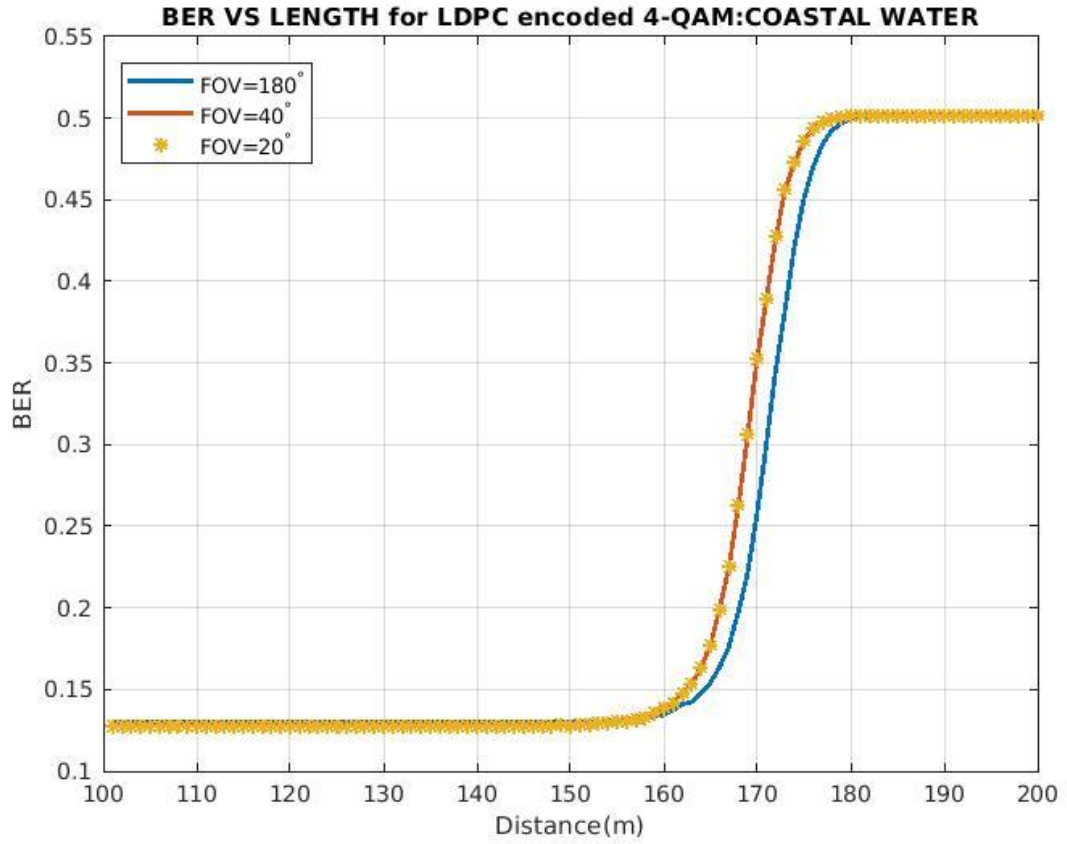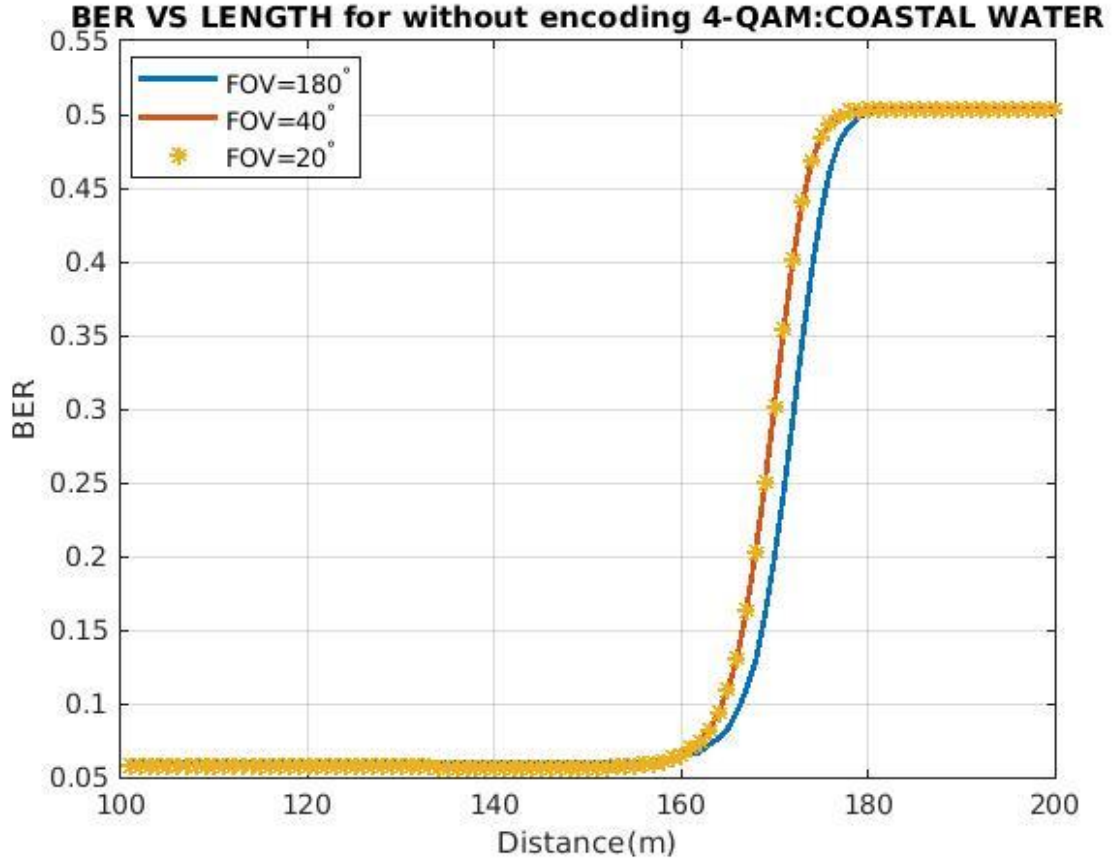
6.2.15. 4-QAM-OFDM IN COASTAL WATER

Fig. 6.20 BER VS LENGTH For 4-QAM without Encoding for Coastal water

In this case, QAM-OFDM modulation of order four is used without any encoding technique. The bit error rate is 0.0601, with a maximum distance of 161.9m. We can see that out of three different Field Of View the transmitting length is maximum for FOV $=180^0$. When we Compare Fig 6.20, Fig 6.19, and Fig 6.18 we can clearly notice that the BCH encoded signal provides the best BER for 4-QAM signal in the coastal water channel.

6.2.16. 4-PSK-OFDM IN COASTAL WATER

BER VS LENGTH for BCH encoded 4-PSK:(COASTAL)

Fig. 6.21 BER VS LENGTH For 4-PSK BCH Encoding for Coastal water

In this case, PSK-OFDM modulation of order four is used with the BCH encoding technique. The bit error rate is 0.0617, with a maximum distance of 4076m. We can see that out of three different Field Of View the transmitting length is maximum for FOV $=180^0$.

6.2.17. 4-PSK-OFDM IN COASTAL WATER

Fig. 6.22 BER VS LENGTH For 4-PSK LDPC Encoding for Coastal water

In this case, PSK-OFDM modulation of order four is used with the LDPC encoding technique. The bit error rate is 0.1231 with a maximum distance of 4076m. We can see that out of three different Field Of View the transmitting length is maximum for FOV $=180^0$
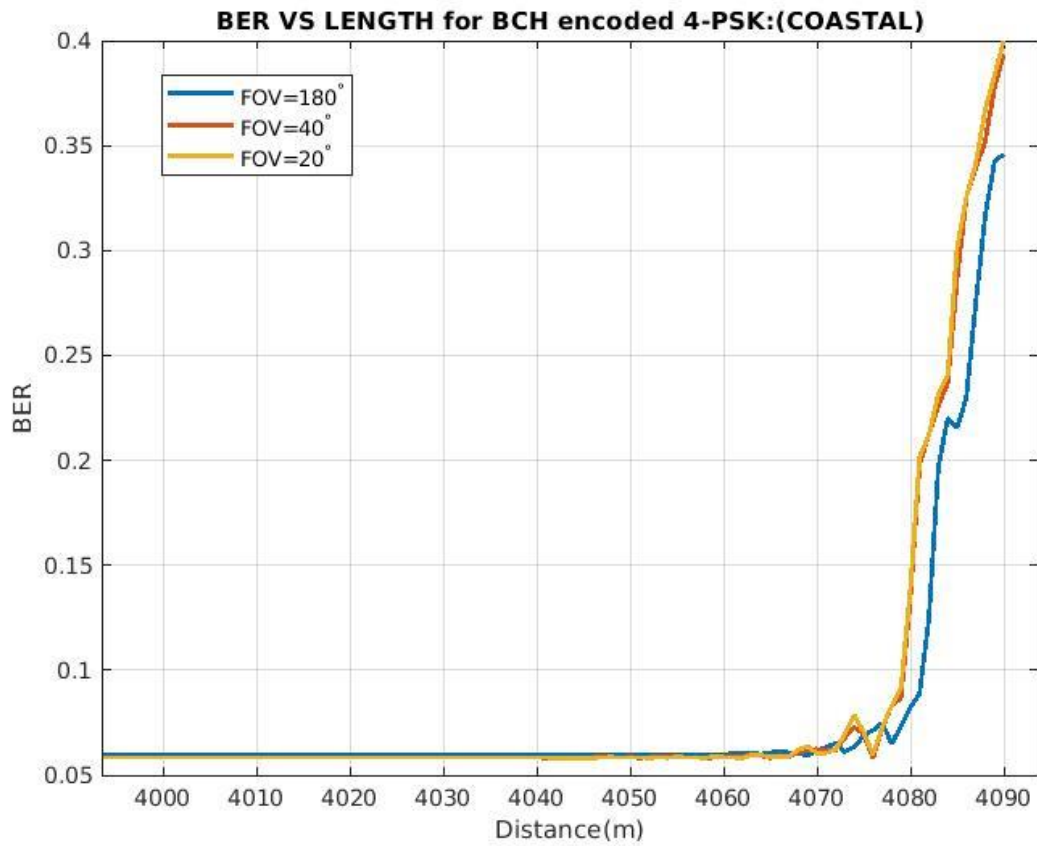
6.2.18. 4-PSK-OFDM IN COASTAL WATER

Fig. 6.23 BER VS LENGTH For 4-PSK without encoding for Coastal water

In this case, PSK-OFDM modulation of order four is used without any encoding technique. The bit error rate is 0.08451, with a maximum distance of 4076m. We can see that out of three different Field Of View the transmitting length is maximum for FOV $=180^0$. When we Compare Fig 6.23, Fig 6.22, and Fig 6.21 we can clearly notice that the BCH encoded signal provides the best BER for 4-PSK signal in the coastal water channel.
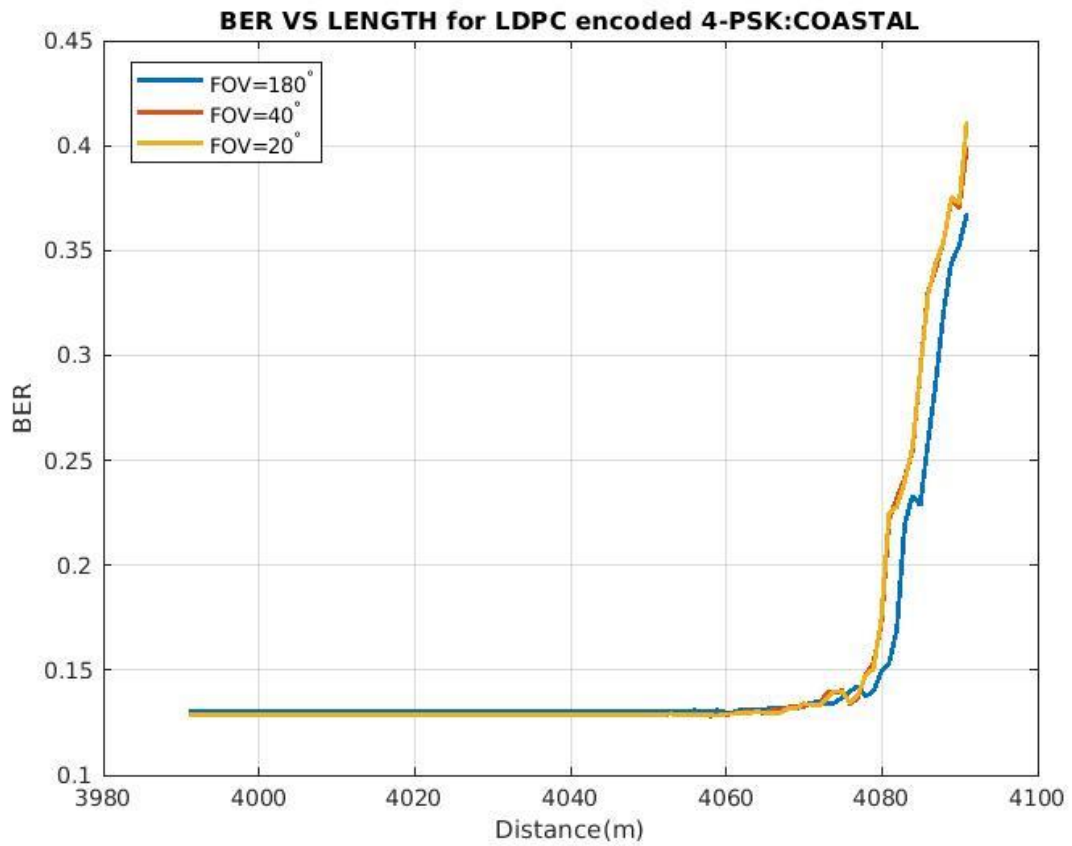
6.2.19. 16-QAM-OFDM IN COASTAL WATER

Fig 6.24 BER VS LENGTH For 16-QAM BCH Encoding for Coastal water

In this case, QAM-OFDM modulation of the order 16 is used with the BCH encoding technique. The bit error rate is 0.2786, with a maximum distance of 161.9m. We can see that out of three different Field Of View the transmitting length is maximum for FOV =180^0
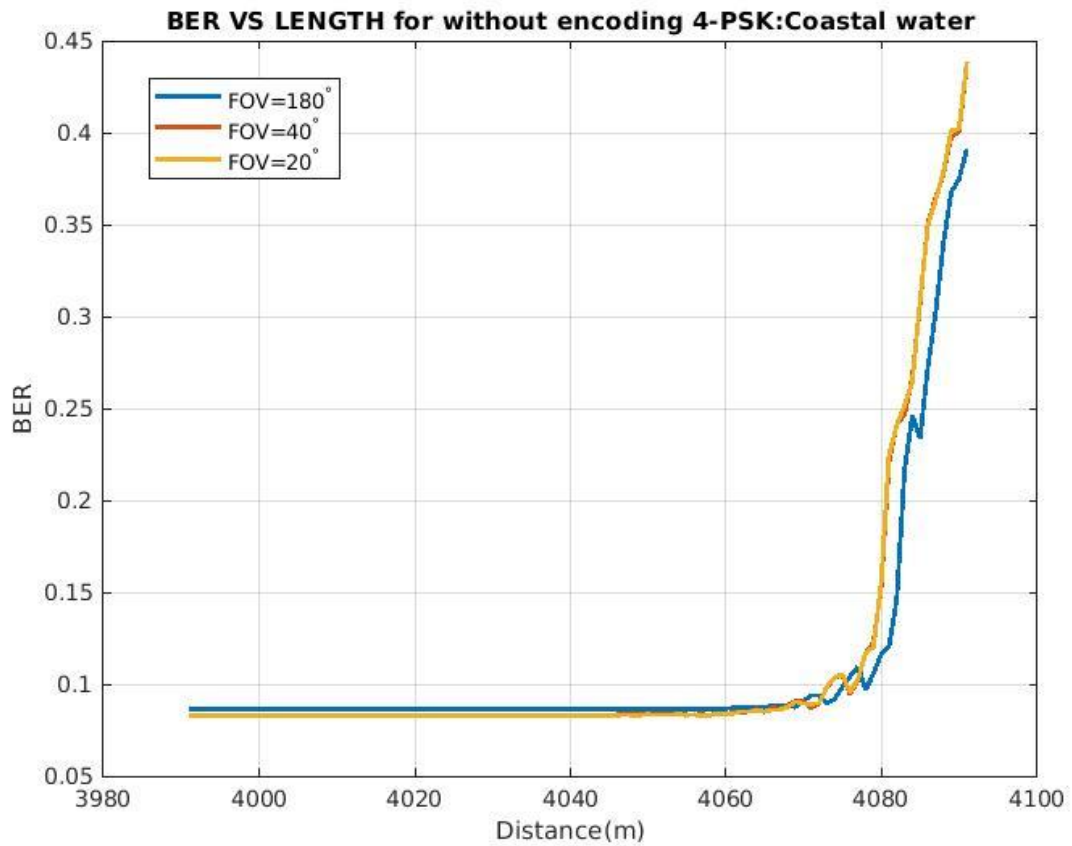
6.2.20. 16-QAM-OFDM IN COASTAL WATER

Fig. 6.25 BER VS LENGTH For 16-QAM LDPC Encoding for Coastal water

In this case, QAM-OFDM modulation of the order 16 is used with the LDPC encoding technique. The bit error rate is 0.49858, with a maximum distance of 161.9m. We can see that out of three different Field Of View the transmitting length is maximum for FOV =180^0

6.2.21. 16-QAM-OFDM IN COASTAL WATER

Fig. 6.26 BER VS LENGTH For 16-QAM without Encoding for Coastal water

In this case, QAM-OFDM modulation of the order 16 is used without any encoding technique. The bit error rate is 0.3099, with a maximum distance of 161.9m. We can see that out of three different Field Of View the transmitting length is maximum for FOV $=180^0$. When we Compare Fig 6.26 ,Fig 6.25, and Fig 6.24 we can clearly notice that the BCH encoded signal provides the best BER for 16-QAM signal in the coastal water channel.
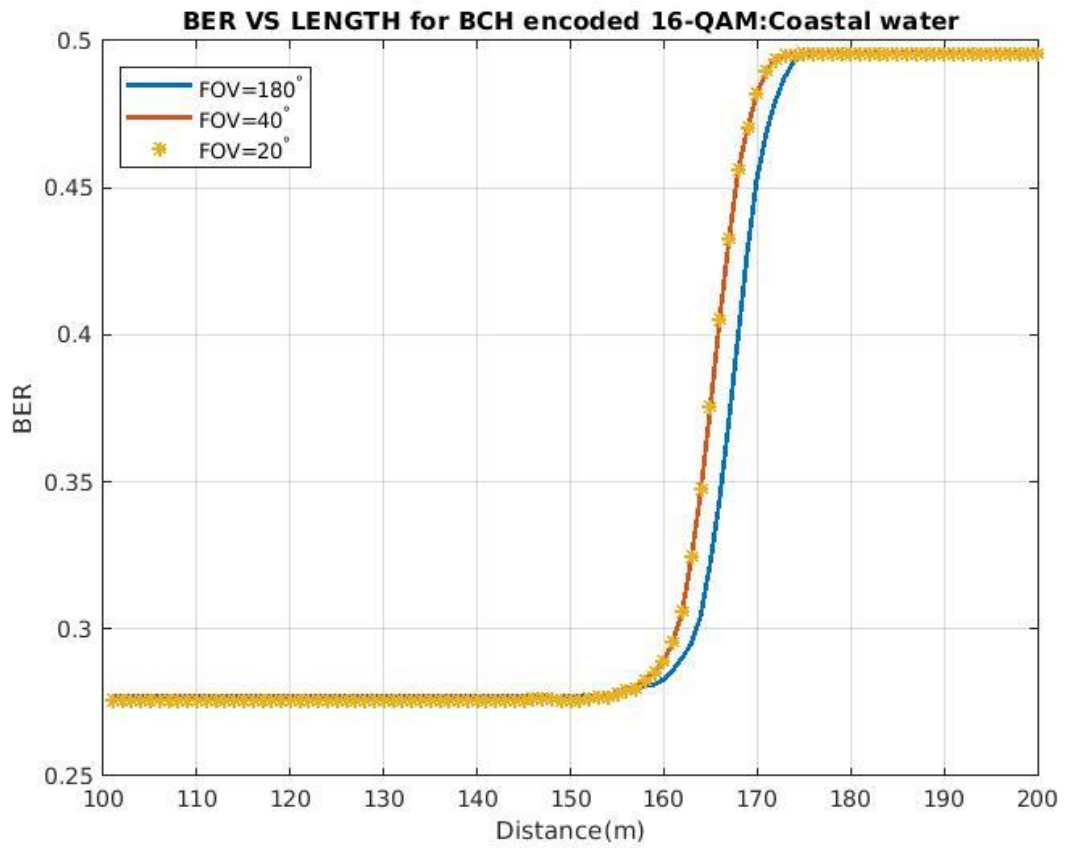
6.2.22. 16-PSK-OFDM IN COASTAL WATER
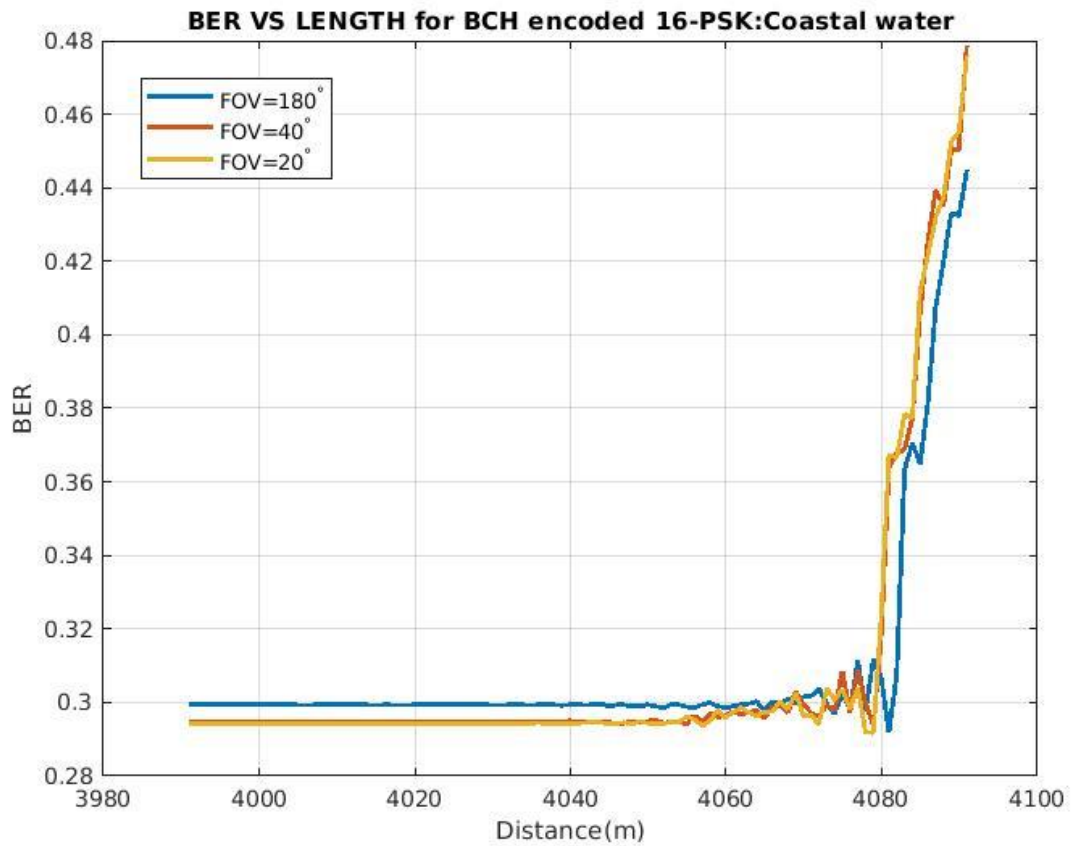
Fig. 6.27 BER VS LENGTH For 16-PSK BCH Encoding for Coastal water

In this case, PSK-OFDM modulation of the order 16 is used with the BCH encoding technique. The bit error rate is 0.3021, with a maximum distance of 4081m. We can see that out of three different Field Of View the transmitting length is maximum for FOV $=180^0$
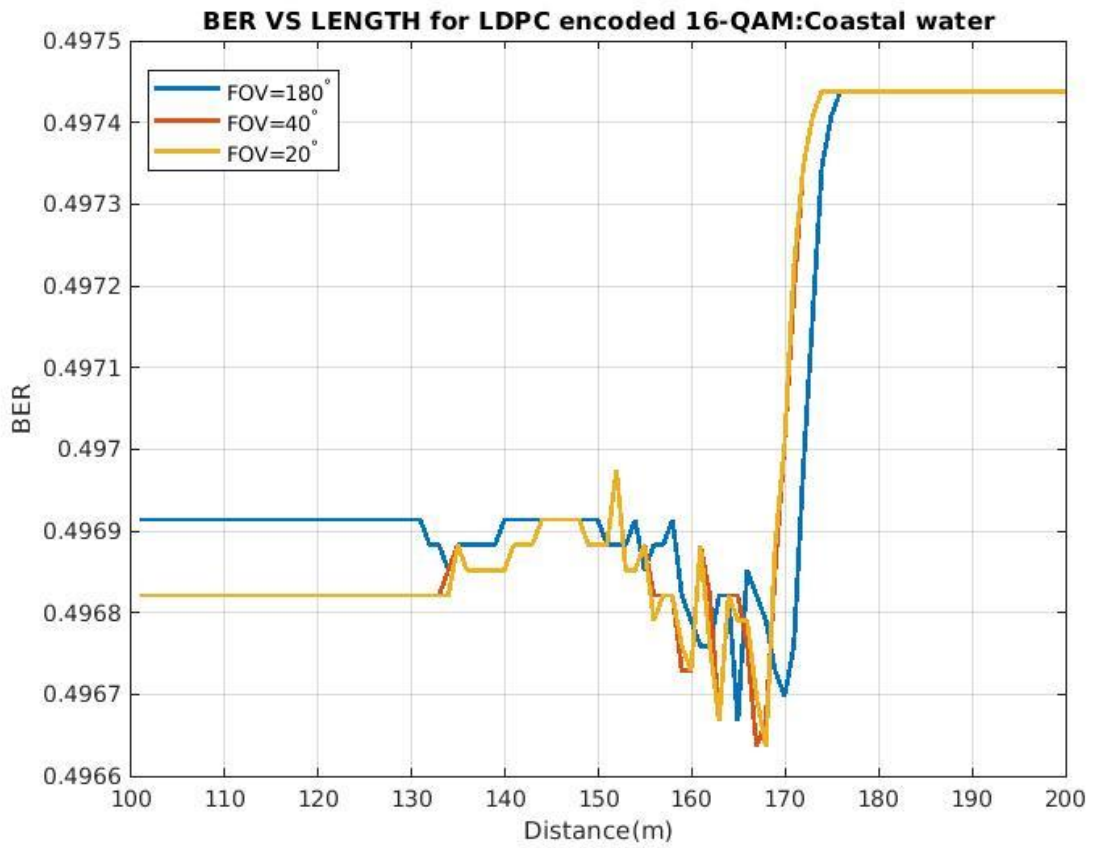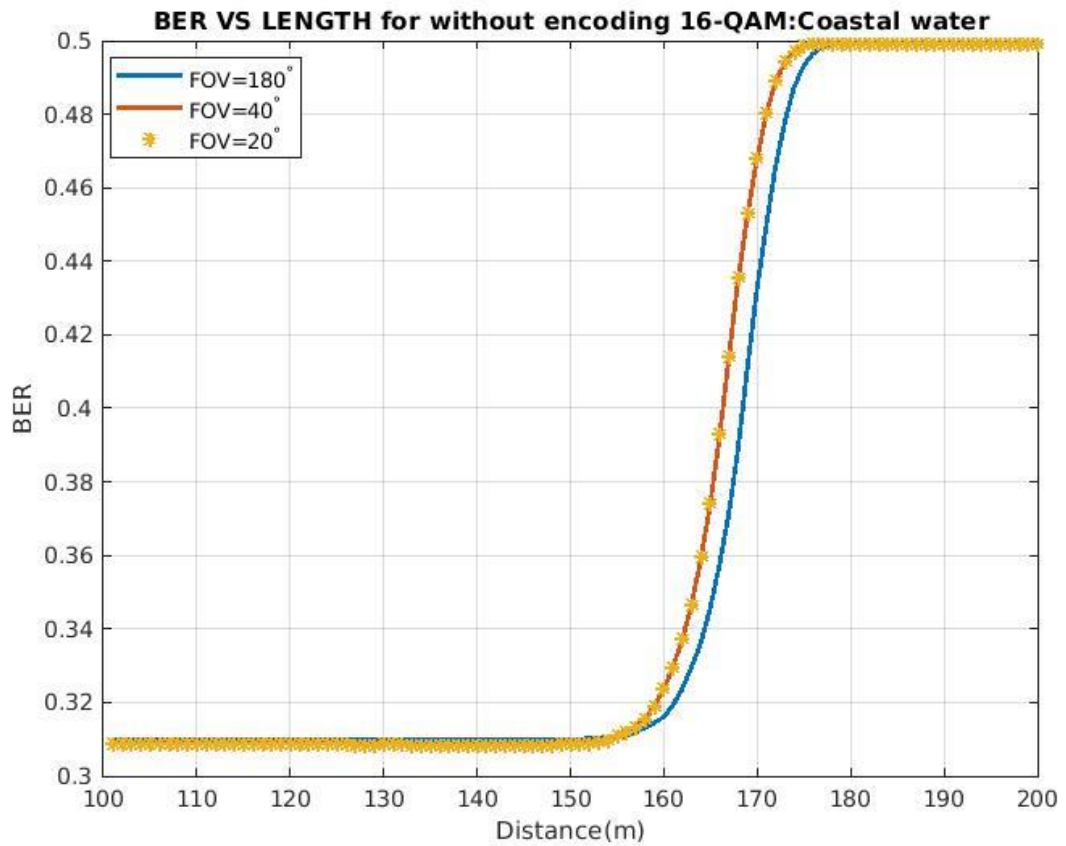
6.2.23. 16-PSK-OFDM IN COASTAL WATER
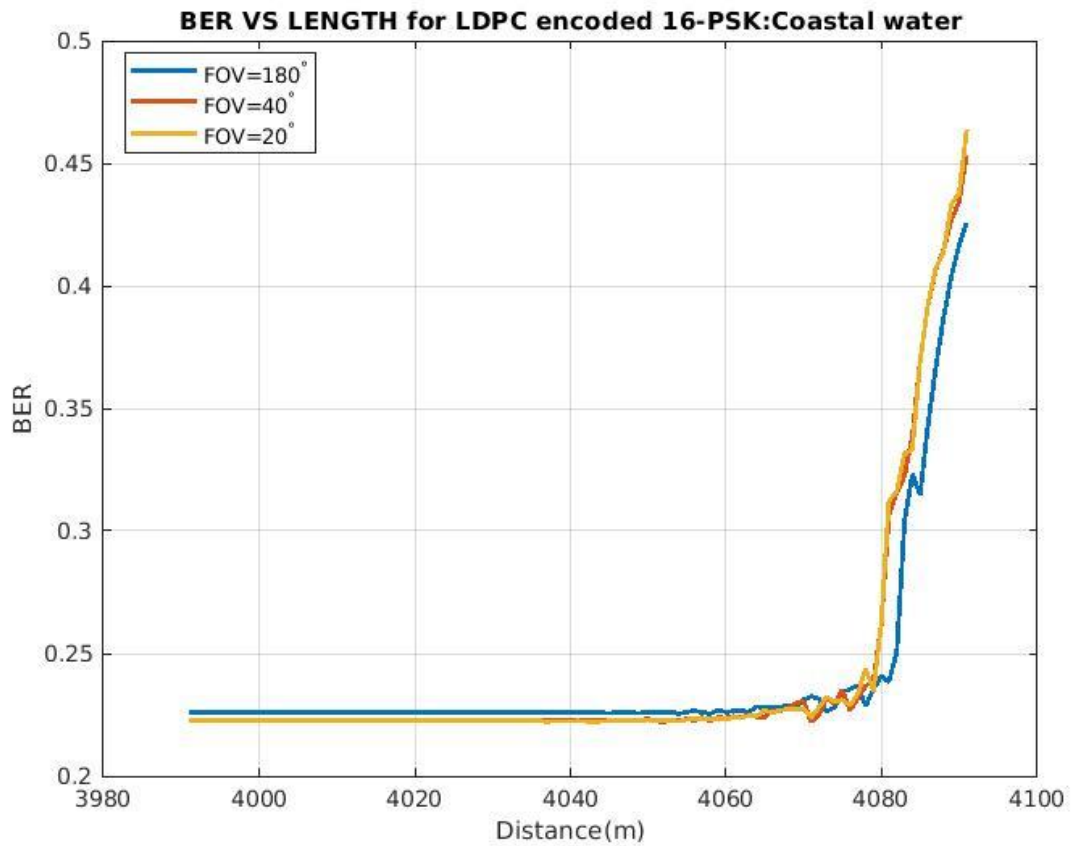
Fig. 6.28 BER VS LENGTH For 16-PSK LDPC Encoding for Coastal water

In this case, PSK-OFDM modulation of the order 16 is used with the LDPC encoding technique. The bit error rate is 0.2264, with a maximum distance of 4081m. We can see that out of three different Field Of View the transmitting length is maximum for FOV =180^0

6.2.24. 16-PSK-OFDM IN COASTAL WATER
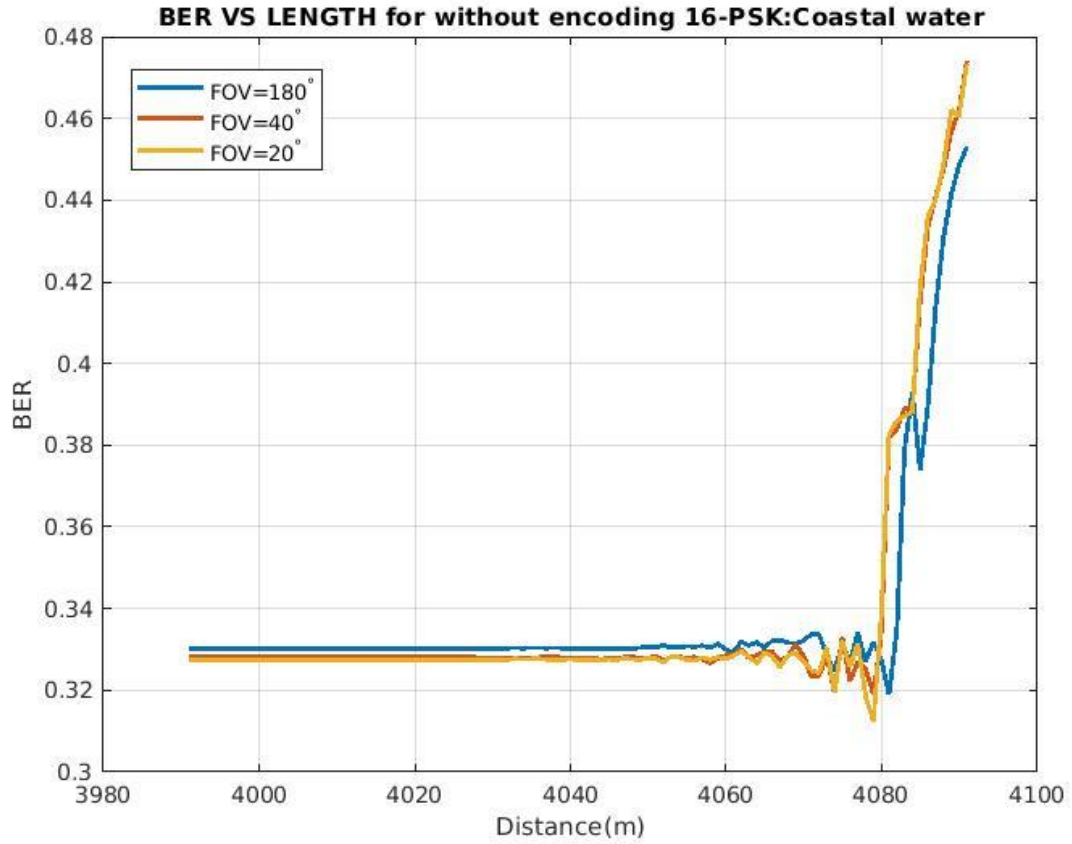
Fig. 6.29 BER VS LENGTH For 16-PSK without Encoding for Coastal water

In this case, PSK-OFDM modulation of the order 16 is used without any encoding technique. The bit error rate is 0.3235, with a maximum distance of 4081m. We can see that out of three different Field Of View the transmitting length is maximum for FOV $=180^0$. When we Compare Fig 6.29 ,Fig 6.28, and Fig 6.27 we can clearly notice that the BCH encoded signal provides the best BER for 16-PSK signal in the coastal water channel.

7. RESULTS

The Table 7.1 lists all the observation madefrom the results and graphs:

Table 7.1 Analysis of bit error rate and channel length for different water types

S. no	Modulation	Modulation order	Encoding	BER(HARBOUR)	BER(COASTAL)	Max.distance(m) HARBOUR	Max.distance(in m) (COASTAL)
1	QAM-OFDM	4	BCH	0.0717	0.0525	62	161.9
2	QAM-OFDM	4	LDPC	0.1739	0.126	62	161.9
3	QAM-OFDM	4	NIL	0.1343	0.0601	62	161.9
4	PSK-OFDM	4	BCH	0.1238	0.0617	1982	4076
5	PSK-OFDM	4	LDPC	0.1739	0.1231	1982	4076
6	PSK-OFDM	4	NIL	0.1725	0.08451	1982	4076
7	QAM-OFDM	16	BCH	0.307	0.2786	62	161.9
8	QAM-OFDM	16	LDPC	0.4919	0.49858	48	161.9
9	QAM-OFDM	16	NIL	0.3378	0.3099	62	161.9
10	PSK-OFDM	16	BCH	0.3615	0.3021	1982	4081
11	PSK-OFDM	16	LDPC	0.2786	0.2264	1982	4081
12	PSK-OFDM	16	NIL	0.3753	0.3235	1982	4081

The above-given observation table has recorded all the results of the simulation that have been executed in this project. This table contains a total of 24 separate combinations of different modulation orders with encoding techniques in two different water channels (i.e., coastal and harbour channel).

As we know that the primary aim of our project is to find out the max length a signal can travel in a channel, and also find out the minimum Bit error rate (BER) a channel offers. Another goal is to find whether Encoding of the signal provides any lower BER to the channel. As far as our aim is considered, the results we obtained are promising and also answers our question that encoding the signal can offer lower BER. However, it is also true that not all encoding techniques provide lower BER for the transmitting signal.

When we look at the results table, we can see that BER is relatively low for BCH encoded signals while comparing it to the non-encoded message signal for their respective counterparts. Even though BER is relatively small, the encoding techniques we used do not provide longer transmitting length than the non-encoded signal. Thus, we can conclude that the Encoding the signal offers low BER, for it does not provide longer transmitting distance.

In the observation table, we can see that there are two separate types of channels are used, coastal and harbour water channel. We can see that the BER is 22% lower for coastal water channels than the harbour water on an average. Furthermore, we can also evidently see that in the coastal channel, the message signal quickly travels almost 61.4% and 51% more length than it travels in the harbour water of QAM and PSK signals, respectively.

In the results, we see that the BER is much higher for the modulation order of 16. that is because with increasing the modulation order, the data rate increases. Hence, we conclude that that BER increases with rising data rates.

One of the abnormal behaviours we observe in the table is that the LDPC encoded signal offers higher BER than the non-encode signals and BCH encoded signal. To justify this behaviour, we have found out that the LDPC code can be recommended as more effective if the signal to noise ratio (SNR) is more significant than 7dB [30] as we know that in coastal water channel that SNR is lower than 7dB. Hence the LDPC encoded signal offers higher BER.

When we compare the results of transmitting length provided by QAM modulation and PSK modulation, we can see that PSK modulation offers nearly 96% more transmitting length than QAM modulation in both Coastal and harbour water channels. Thus, we can conclude that PSK provides a more significant transmitting length than it is being supplied by QAM modulation.

One interesting behaviour noted in the BER vs Distance graph is that, the BER did not increase gradually with increasing distance as anyone would expect, but instead it stayed constant until the channel capacity reached and then exponentially reached its maximum value. This behaviour can also be seen in [31]

8. CONCLUSION

In this project, we have modelled an underwater channel response for Harbour and coastal water. Then we have analyzed the BER vs Length performance for these different Underwater wireless channel types. We have transmitted several signals with varying combinations of mapping schemes and error correction codes with different modulation orders. After all the simulations, it is quite clear that any signal transmitted in an underwater wireless channel suffers substantial attenuation due to parameters like absorption and scattering. This is a drawback. However, according to our findings in Table 7.1, the maximum transmitting distance, a signal can travel is varying from 48m-4076m. The maximum distance we achieved in Underwater channel with the lowest BER is 4-PSK signal encoded with BCH error correction code is 4076m at FOV=180^0 in a coastal water channel. This distance is up-and-coming, where it can be used for various applications like Unmanned underwater vehicles, submarines, ships, and underwater sensors. We can also deploy this to gather essential data such as real-time videos environmental and security data, which may be time sensitive[32].However according to recent findings the maximum estimated distances of 144 m and 117 m with corresponding BERs of 1.89×10^{-3} and 5.31×10^{-4} at were acquired in UWOC system using on-off keying (OOK) modulation scheme, respectively[33], and also , Sonardyne has commercialized the BlueComm UWOC system which can operate over distances of up to 200 m [7], and 16-QAM OFDM signal travel 10.2 m with BER of 2.4×10^{-3} in a seawater channel[31], comparing to these data, the results we obtained is very reassuring that Underwater wireless channel has very high potential.

However, in this project, we have deployed only error correction codes like LDPC and BCH to control bit error rate. We have not used equalization techniques like Volterra or least mean square methods to control error. We further propose to incorporate different equalization techniques to enhance the performance of our system. Using these methods the bit-error rate can be brought down by a significant number, and it also possible to increase the transmitting length.

REFERENCES:

[1] Yiming Li, Mark S. Leeson, and Xiaofeng Li, "Impulse response modeling for underwater optical wireless channels," (2018) Appl. Optical society of America 57, pp.4815-4823

[2] J. Lloret, S. Sendra, M. Ardid, and J. J. P. C. Rodrigues, "Underwater Wireless Sensor Communications in the 2.4 GHz ISM Frequency Band," Sensors, vol. 12, no. 4, pp. 4237–4264, Mar. 2012.

[3] B. Cochenour, L. Mullen, A. Laux, and T. Curran, "Effects of Multiple Scattering on the Implementation of an Underwater Wireless Optical Communications Link," OCEANS 2006, Boston, MA, 2006, pp. 1-6, DOI: 10.1109/OCEANS.2006.306863.

[4] Yoong, Hou Pin, Kiam Beng Yeo, Kenneth Tze Kin Teo, and Wei Loong Wong. "Underwater wireless communication system: Acoustic channel modeling and carry frequency identification." (2009) International Journal of Simulation, Systems, Science and Technology 13, no. 3C:pp. 1-6.

[5] Kumar, P.V., Praneeth, S.S.K. and Narender, R.B.,. "Analysis of optical wireless communication for underwater wireless communication". (2011) International Journal of Scientific & Engineering Research, 2(6), pp.194-202.

[6] Mohamed, A.E.N.A., Rashed, A.N.Z. and El-Nabawy, A.E.,. "Under water optical wireless communications technology for short and very short ranges". (2012)IJ Information Technology and Computer Science, 5, pp.46-57.

[7] M. Khalighi, C. Gabriel, T. Hamza, S. Bourennane, P. Léon, and V. Rigaud, "Underwater wireless optical communication; recent advances and remaining challenges," 2014 16th International Conference on Transparent Optical Networks (ICTON), Graz, 2014, pp. 1-4, DOI: 10.1109/ICTON.2014.6876673.

[8] P. Kumar, V. K. Trivedi, and P. Kumar, "Recent trends in multi-carrier underwater acoustic communications," 2015 IEEE Underwater Technology (UT), Chennai, 2015, pp. 1-8, DOI: 10.1109/UT.2015.7108313.

[9] Anandalatchoumy, S. and Sivaradje, G." Comprehensive study of acoustic channel models for underwater wireless communication networks".(2015) International Journal on Cybernetics & Informatics, 4(2), pp.227-240.

[10] Jagadeesh, V.K., Naveen, K.V. and Muthuchidambaranathan, P., 2015. "BER performance of NLOS underwater wireless optical communication with multiple scattering". Int. J. Res. Schol. Innov, 9(2), pp.562-566.

[11] Gussen, C.M., Diniz, P.S., Campos, M.L., Martins, W.A., Costa, F.M. and Gois, J.N., 2016. A survey of underwater wireless communication technologies. J. Commun. Inf. Sys., 31(1), pp.242-255.

[12] H. Kaushal and G. Kaddoum, "Underwater Optical Wireless Communication," in IEEE Access, vol. 4, pp. 1518-1547, 2016, DOI: 10.1109/ACCESS.2016.2552538.

[13] Huihui Zhang, Yuhan Dong. (2016). "General Stochastic Channel Model and Performance Evaluation for Underwater Wireless Optical Links" in IEEE Transactions on Wireless Communications (Volume: 15 , Issue: 2 , Feb. 2016); Page(s): 1162 – 1173; INSPEC Accession Number: 15785893; DOI: 10.1109/TWC.2015.2485990

[14] Xueyi Geng ; Adam Zielinski. (2002). "An eigenpath underwater acoustic communication channel model". Published in 'Challenges of Our Changing Global Environment'. Conference Proceedings. OCEANS '95 MTS/IEEE, Publisher: IEEE, DOI: 10.1109/OCEANS.1995.528591; INSPEC Accession Number: 5225669, Conference Location: San Diego, California, USA.

[15] R. Galvin, R.E.W. Coats. (2002). "A stochastic underwater acoustic channel model". Published in: OCEANS 96 MTS/IEEE Conference Proceedings. The Coastal Ocean - Prospects for the 21st Century, DOI: 10.1109/OCEANS.1996.572599, Publisher: IEEE, Conference Location: Fort Lauderdale, FL, USA.

[16] Albert F. Harris, Michele Zorzi. (2007). "Modeling the underwater acoustic channel in ns2", Publication: ValueTools '07: Proceedings of the 2nd international conference on Performance evaluation methodologies and tools, October 2007, Article No.: 18, Pages 1–8.

[17] Hassan Makine Oubei, Emna Zedini, Rami T. ElAfandy, Abla Kammoun, Mohamed Abdallah, Tien Khee Ng, Mounir Hamdi, Mohamed-Slim Alouini, and Boon S. Ooi. (2017). "Simple statistical channel model for weak temperature-induced turbulence in underwater wireless optical communication systems". Vol. 42, Issue 13, pp. 2455-2458. Publisher: Optical Society of America.

[18] F. De Rango ; F. Veltri ; P. Fazio. (2012). "A multipath fading channel model for underwater shallow acoustic communications". Published in: 2012 IEEE International Conference on Communications (ICC). Publisher: IEEE, DOI: 10.1109/ICC.2012.6364590, Conference Location: Ottawa, ON, Canada.

[19] Christian R. Berger, Shengli Zhou, James C. Preisig , Peter Willett. (2009). "Sparse Channel Estimation for Multicarrier Underwater Acoustic Communication: From Subspace Methods to Compressed Sensing". Published in: IEEE Transactions on Signal Processing (Volume: 58, Issue: 3, March 2010). Publisher: IEEE. Page(s): 1708 – 1721, DOI: 10.1109/TSP.2009.2038424.

[20] Sermsak Jaruwatanadilok. (2008). "Underwater Wireless Optical Communication Channel Modeling and Performance Evaluation using Vector Radiative Transfer Theory". Published in: IEEE Journal on Selected Areas in Communications (Volume: 26, Issue: 9, December 2008). Publisher: IEEE, Page(s): 1620 – 1627, DOI: 10.1109/JSAC.2008.081202.

[21] Guoqing Zhou ; Taebo Shim. (2008). "Simulation Analysis of High Speed Underwater Acoustic Communication Based on a Statistical Channel Model". Published in: 2008 Congress on Image and Signal Processing. Publisher: IEEE, DOI: 10.1109/CISP.2008.85, Conference Location: Sanya, Hainan, China.

[22] Chengsheng Pan, Liangchen Jia, Ruiyan Cai, and Yuanming Ding. (2011). "MODELING AND SIMULATION OF CHANNEL FOR UNDERWATER COMMUNICATION NETWORK". International Journal of Innovative Computing, Information and Control, Volume 8, Number 3(B), March 2012. School of Information Engineering Dalian University Economic and Technological Development Zone, Dalian 116622, P. R. China.

[23] Laura J. Johnson, Roger J. Green, and Mark S. Leeson. (2013). "Underwater optical wireless communications: depth dependent variations in attenuation". Vol. 52, Issue 33, pp. 7867-7873 (2013), Publisher: Optical Society of America.

[24] Johnson, Laura J; Jasman, Faezah; Green, Roger J; Leeson, Mark S. (2014). "Recent advances in underwater optical wireless communications". Source: Underwater Technology, Volume 32, Number 3, November 2014, pp. 167-175(9), Publisher: Society for Underwater Technology.

[25] Shlomi Arnon and Debbie Kedar. (2009). "Non-line-of-sight underwater optical wireless communication network". Vol. 26, Issue 3, pp. 530-539, (2009), DOI: https://doi.org/10.1364/JOSAA.26.000530

[26] Weihao Liu ; Difan Zou ; Peilin Wang ; Zhengyuan Xu ; Liuqing Yang. (2014). "Wavelength dependent channel characterization for underwater optical wireless communications". Published in: 2014 IEEE International Conference on Signal Processing, Communications and Computing (ICSPCC), Publisher: IEEE, DOI: 10.1109/ICSPCC.2014.6986327, Conference Location: Guilin, China.

[27] Laura Johnson, Roger Green, Mark Leeson. (2013). "A survey of channel models for underwater optical wireless communication". Published in: 2013 2nd International Workshop on Optical Wireless Communications (IWOW). Publisher: IEEE, DOI: 10.1109/IWOW.2013.6777765, Conference Location: Newcastle upon Tyne, UK.

[28] Ahmed Nabih Zaki Rashed & Hamdy A. Sharshar. (2013). "Performance Evaluation of Short Range Underwater Optical Wireless Communications for Different Ocean Water Types". Wireless Personal Communications volume 72, pages693–708(2013).

[29] Zabih Ghassemlooy ; Shlomi Arnon ; Murat Uysal ; Zhengyuan Xu ; Julian Cheng. (2015). "Emerging Optical Wireless Communications-Advances and Challenges". Published in: IEEE Journal on Selected Areas in Communications (Volume: 33, Issue: 9, Sept. 2015). Publisher: IEEE. DOI: 10.1109/JSAC.2015.2458511. Page(s): 1738 – 1749.

[30] Uryvsky, L.O. and Osypchuk, S.O., (2014). "Comparative analysis of LDPC and BCH codes error-correcting capabilities." Published in: Information and telecommunication sciences (pp. 5-9)

[31] Wu TC, Chi YC, Wang HY, Tsai CT, Lin GR. Blue laser diode enables underwater communication at 12.4 Gbps. Sci. Rep. 2017;7:40480. doi: 10.1038/srep40480

[32] S. Jaruwatanadilok, "Underwater Wireless Optical Communication Channel Modeling and Performance Evaluation using Vector Radiative Transfer Theory," in IEEE Journal on Selected Areas in Communications, vol. 26, no. 9, pp. 1620-1627, December 2008, DOI: 10.1109/JSAC.2008.081202.

[33] H. Chen et al., "Toward Long-Distance Underwater Wireless Optical Communication Based on A High-Sensitivity Single Photon Avalanche Diode," in IEEE Photonics Journal, vol. 12, no. 3, pp. 1-10, June 2020, Art no. 7902510, doi: 10.1109/JPHOT.2020.2985205.